COMBINED LOCAL AND OVERALL BUCKLING OF RECTANGULAR THIN-WALLED TUBULAR COLUMNS

BY

JACQUES COHEN

B.S., Universidade de Minas Gerais, Brazil, 1955
M.S., University of Florida, 1958

THESIS

SUBMITTED IN PARTIAL FULFILLMENT OF THE REQUIREMENTS
FOR THE DEGREE OF DOCTOR OF PHILOSOPHY IN CIVIL ENGINEERING
IN THE GRADUATE COLLEGE OF THE
UNIVERSITY OF ILLINOIS, 1960

URBANA, ILLINOIS

UNIVERSITY OF ILLINOIS

THE GRADUATE COLLEGE

July 19, 1960

I HEREBY RECOMMEND THAT THE THESIS PREPARED UNDER MY SUPERVISION BY JACQUES COHEN

ENTITLED COMBINED LOCAL AND OVERALL BUCKLING OF RECTANGULAR THIN-WALLED TUBULAR COLUMNS

BE ACCEPTED IN PARTIAL FULFILLMENT OF THE REQUIREMENTS FOR THE DEGREE OF DOCTOR OF PHILOSOPHY IN CIVIL ENGINEERING

H. N. Trumpler
In Charge of Thesis

J. B. Breen
Head of Department

Recommendation concurred in†

E. A. Witmer
James O. Smith
Jean Cornelle
C. P. Siess

Committee on Final Examination†

† Required for doctor's degree but not for master's.

D517

ACKNOWLEDGMENT

The author wishes to express his sincere appreciation to the members of his doctoral committee for their helpful suggestions. In particular, acknowledgment is made to Professor J. E. Duberg for suggesting the topic and to Professor W. H. Munse, Chairman of the Committee, for the encouragement and assistance given throughout this investigation.

TABLE OF CONTENTS

SUMMARY

The Rayleigh-Ritz procedure has been applied to the study of the combined action, within the elastic range, of local and overall buckling of rectangular thin-walled tubular columns. The selection of the analytical expression for the assumed deflected shape has been based on existing solutions for plate and column action considered individually. The minimization of the total energy of the column leads to a system of nonlinear simultaneous algebraic equations which are solved numerically by a high-speed digital computer.

The results are presented in diagrams showing the variation of the important generalized coordinates with the applied load.

I INTRODUCTION

1. Statement of Problem

It is well known that the critical load* of an elastic column is linearly proportional to the modulus of elasticity of the column material. After the critical load is reached the column undergoes large deflections at the same level of applied load. In the theory of small deflections of columns this represents the limiting load to which the member can be subjected.

A plate with simply supported edges exhibits a basically different behavior. After the critical load is reached and large lateral deflections have taken place, the plate is still able to carry additional load with an apparent modulus of elasticity** which is smaller than Young's modulus.

In the case of thin-walled columns, the component plates may buckle locally at an early stage of the loading and still carry additional load. Very little information is available concerning the effect of plate buckling on the overall buckling of the columns. The present investigation attempts to further clarify this matter by studying the interaction of local and overall column buckling of a thin-walled rectangular tube.

---

* The term critical load is used to denote the load at which a perfectly straight column or plate start to deflect laterally.

** The apparent modulus of elasticity is defined as the slope of the curve representing load versus displacement of the point of application of the load.

2. Object and Scope of Investigation

This study is a theoretical analysis, within the elastic range, of the behavior of an axially loaded thin-walled rectangular tube. Since no real structural element is perfectly straight it is desirable to assume initial eccentricities in both column and component plates so that their effect on the behavior of an actual structure may be studied. The behavior of a perfectly straight column may be inferred by considering the limiting case in which the initial eccentricities tend to zero.

The basic equations have been derived herein for columns with arbitrary dimensions under the assumption that the side plates* do not buckle. The method of analysis is developed to consider the combined action of local and column buckling, in particular the effects of different geometries and small initial imperfections in both column and component plates.

The study is such that it is perhaps most useful as a research tool, and it is certainly not intended for direct use in routine design. The method has been applied to a limited number of cases so that only general qualitative conclusions can be drawn; an exhaustive study of the variables involved is beyond the scope of the present study.

3. Historical Review

The basic differential equation of elastic column buckling, in the case of small lateral deflections, was derived by Euler in the eighteenth century. The buckling and post-buckling analyses of plates are comparatively new subjects that, in recent years, have attracted the attention of numerous in-

---

* Plates AC and BD in Fig. 1.

vestigators. This interest has arisen due to the increasing importance of light-weight structures and has been stimulated by the development of more suitable means for solving the involved nonlinear differential equations encountered in the theory of large deflections of plates. The nonlinearity of the equations originates from the fact that, in the case of large deflections, the normal displacements of the plate have an effect on the membrane stresses; this interaction leads to nonlinear terms in the equilibrium equations of the plate element.

Some of the most important investigations concerning the post-buckling behavior of plates are described in references (2)* through (9). The basic differential equations for a plate undergoing large deflections were originally derived by von Karman and have been transcribed by Timoshenko (3); the concept of effective width was introduced by von Karman, Sechler, and Donnell (4). Approximate solutions for post-buckling behavior were presented by Timoshenko (3) and Marguerre (2), whose analyses were carried out by energy methods. Levy (5) used a Fourier series expansion to obtain the solution to the large deflection equations for plates. Hu, Lundquist, and Batdorf (6) and also Coan (7) have investigated the effects of small imperfections in square plates. Mayers and Budiansky (8) studied the behavior of a flat square plate compressed beyond the elastic buckling load into the plastic range. Stein (9) linearized the nonlinear differential equations by expanding the displacements in power series and studied the change of the buckle pattern in rectangular plates.

According to all of the above mentioned analyses, there is a marked change in the apparent modulus of elasticity after the plates buckle. Marguerre

---

* Numbers in parentheses, unless otherwise designated, refer to references listed in the bibliography.

(2) found that for a simply supported plate the apparent modulus of elasticity, in the early post-buckling range, is one half of Young's modulus. This implies that the problem of the combined action of local and column buckling in thin-walled rectangular tubes resembles that of the behavior of columns made of material exhibiting a nonlinear stress-strain diagram. The latter problem was discussed by Engesser and von Karman (2) early in this century, approximately one hundred and fifty years after Euler s development of the elastic column theory. No further major development was made in this field until 1948 when Shanley (2) questioned the validity of von Karman's assumptions and formulated his theory of columns in the inelastic range. Subsequently various investigators, among them Duberg and Wilder (10), verified analytically the validity of Shanley's theory by working with idealized column models. References (1) and (2) contain extensive reviews of the historical development of column and plate buckling.

In contrast with the large number of publications concerning column and plate action individually, there are very few references which consider the combined action of local and column buckling. Bijlaard and Fisher (11 and 12), using an approximate method (collocation), derived expressions for the column strength of H-sections and square tubes in the post-buckling range of the component plates.

II METHOD OF ANALYSIS

4. Method of Solution

The Rayleigh-Ritz method* has been selected for solving the present problem. The main reason for this selection is the fact that solutions by this method are available for the limiting cases, i.e. plate and column action individually. Furthermore, this method yields equations that are particularly amenable to solution by a high-speed digital computer.

According to the Rayleigh-Ritz procedure an elastic system with an infinite number of degrees of freedom is reduced to a discrete system by means of assumptions about the nature of the deformation. The assumed deflected shape is expressed analytically in terms of selected generalized coordinates, usually the coefficients of a Fourier series expansion. These generalized coordinates are determined by minimization of the total energy of the system. This procedure leads to an upper bound solution of the problem, when considering a limited number of generalized coordinates. The larger the number of properly selected coordinates, the higher is the accuracy that can be expected; however the labor involved in the computations increases enormously with the number of coordinates. It is therefore of utmost importance to make a judicious selection of the generalized coordinates so as to reduce their number to a minimum without excessively reducing the accuracy of the solution. Such a selection can be accomplished by studying existing solutions for the limiting cases.

The introduction of initial eccentricities in both plate and column transforms the buckling problem (eigenvalue) into a stress analysis. The crit-

---

* For detailed explanation and examples of application refer to Timoshenko (3) and Bleich (2).

ical load, i.e. the load representing a bifurcation point in the configuration space* of the system, can be determined by gradually reducing the initial eccentricities to zero. This method is usually referred to as the imperfection theory of buckling (13).

5. Basic Assumptions

The assumptions involved in this analysis may be stated as follows:

(a) The column material is homogeneous, elastic and isotropic.

(b) The lateral deflections of the column are small so that the usual approximate expression for the radius of curvature remains applicable; however a large deflection theory is used to treat the plate buckling.

(c) Normals to the column axis or axes of the plates remain normal after deformation.

(d) The component plates are assumed to be simply supported along the edges, which are free to move laterally and remain straight after plate buckling has taken place.

(e) The side plates do not buckle (plates AC and BD in Fig. 1).

(f) The ends of the column are free to rotate.

(g) Poisson's ratio is assumed to be equal to zero.

Assumptions (a), (b), (c), and (f) are the basis of the theory of small deflections of elastic columns. Assumption (d) is conservative since in the case of an actual tube the continuity at the edges causes a rotational restraint in the flange plates (plates AB and CD in Fig. 1). Appendices I and II, where plate and column action are studied separately, indicate that Poisson's ratio does

---

* Refer to Langhaar (13).

not have a significant effect on the displacements. Consequently, it may be expected that assumption (g) does not introduce appreciable errors in the present analysis.

6. Notations

The following notations have been adopted for use in this study:

b, b_1	Column width as indicated in Fig. 1.
g	Generalized coordinate.
i, j	Used as subscript to denote the ith variable x_i and the jth function F_j; i is also used as a subscript to denote initial eccentricity in Chapter II; j is used as a superscript to denote the component plates 1, 2, 3, and 4 shown in Fig. 1.
n	Number of square buckle waves; also used as a subscript to denote the nth variable x_n or the nth function F_n.
t, t_1	Plate thickness as indicated in Fig. 1.
$x_1, x_2, \ldots, x_i, \ldots, x_n$	Unknowns; in the present problem they stand for generalized coordinates expressed in a dimensionless form.
Δx_i	Increments of the unknowns x_i.
x_i'	Corrected values of unknowns x_i.
x, y, z	Cartesian coordinates oriented as shown in Fig. 1.
u, v, w	Displacements in the x, y, and z directions measured from the undeformed position; used with subscripts to denote generalized coordinates.
u_0	Column shortening.
u_{cr}^{pl}	Plate critical shortening for $\nu = 0$, i.e. $\frac{\pi^2}{3}\frac{t^2}{b^2}$.

w_{0i}	Initial eccentricity of the column axis.
w_{1i}	Initial eccentricity of the plate axis.
w_0	Central deflection of the column axis.
w_a, w_b	Buckle crest deflection in the compression and tension flange respectively.
A	Column cross sectional area.
D	Flexural rigidity, i.e. $\frac{Et^3}{12(1-\nu^2)}$.
E	Young's modulus.
$F_1, F_2, \ldots, F_j, \ldots, F_n$	Functions of variables $x_1, x_2, \ldots, x_i, \ldots, x_n$.
H, I, J, K	Dimensionless parameters defined by Eqs. 15.
I_f	Moment of inertia of the flanges with respect to axis R-R in Fig. 1.
I_t	Moment of inertia of the column cross section with respect to axis R-R in Fig. 1.
L	Column length.
T_a, T_b, T_c	Functions of w and w_i as given by Eq. 11.
V_B	Strain energy of bending.
V_S	Strain energy of membrane stresses.
V_P	Potential energy.
V_T	Total energy.
α	Infinitesimal quantity; equal to 10^{-7} in the present analysis.
ϵ_x, ϵ_y, ϵ_z	Strains in the x, y, and z directions.
γ_{xy}, γ_{yz}, γ_{zx}	Shearing strains in the xy, yz, and zx planes
σ	Applied stress.
$\Delta\sigma$	Applied stress increment; equal to $\frac{1}{40}\sigma_E$ in the present analysis.

σ_{cr}^{pl}	Plate critical stress for $\nu = 0$, i.e. $\frac{\pi^2}{3} \frac{t^2}{b^2} E$.
σ_E	Euler stress, i.e. $\pi^2 \frac{EI_t}{AL^2}$.
σ_{max}	Maximum stress that can be applied to the column.
λ	Slenderness, i.e. $L/\sqrt{I_t/A}$.
ν	Poisson's ratio.

Superscripts in parentheses denote the component plates as indicated in Fig. 1.

7. Theory

A half sine wave is frequently used to express mathematically the longitudinal imperfection of an initially eccentric column. Similarly, a half sine wave is also used to represent the initial shape of a plate in both longitudinal and transverse directions. Hu, Lundquist, and Batdorf have used this shape of initial imperfection in their study of the effect of small deviations from flatness on the post-buckling behavior of plates. This same shape of initial eccentricities has been assumed in the present analysis which may then be checked, in the limiting cases, with more accurate solutions (see Appendices I and II).

The selection of the shape expressing the lateral deflections of the rectangular tube and component plates may also be accomplished by studying separately the existing solutions for plate and column action. A half sine wave is known to represent the exact buckled shape of the axis of an elastic column hinged at both ends. Even when the stress-strain diagram for the column material is nonlinear — a problem that, as stated previously, resembles the present case — a sine curve is still a good approximation for the deflected shape (10). Numerous investigators (2, 3, and 8) have used the surface generated by half sine waves in the transverse and longitudinal directions to express the buckled shape of a plate simply supported along all edges. The validity of

such an assumption is confirmed by more refined analyses (6 and 7), particularly in the early post-buckling range.

The choice of the deflected shape in the plane of the plates represents a critical factor in this analysis. They should be selected so as to reduce the middle surface strains to a minimum. The importance of the preceding remark is explained in reference (14), from which the following passage is quoted: "The membrane strains that accompany buckling are small, since large membrane strains cause excessive strain energy. This fact is exemplified if we deform a piece of sheet metal in our hands. Although we can bend it easily we cannot stretch it noticeably... Loosely speaking the 'easiest' way for a shell to buckle is that which entails the smallest membrane strains."

The approximate membrane strains are given (3) by,

$$\begin{aligned} \epsilon_x &= \frac{\partial u}{\partial x} + \frac{1}{2}\left(\frac{\partial w}{\partial x}\right)^2 \\ \epsilon_y &= \frac{\partial v}{\partial y} + \frac{1}{2}\left(\frac{\partial w}{\partial y}\right)^2 \end{aligned} \qquad (1)$$

If the expressions for the u and v displacements are chosen so that $\frac{\partial u}{\partial x}$ and $\frac{\partial v}{\partial y}$ have the same shape as $\frac{1}{2}\left(\frac{\partial w}{\partial x}\right)^2$ and $\frac{1}{2}\left(\frac{\partial w}{\partial y}\right)^2$, a minimum of strain energy due to membrane stresses may be expected when using Rayleigh-Ritz's procedure. This has been the basis for selection of the u and v terms in the present analysis.

In view of the foregoing, the assumed deflected shape is given by (see Figs. 1 and 2),

$$\begin{cases} w^{(1)} = w_0 \sin\frac{\pi x}{L} - w_a \sin\frac{n\pi x}{L} \sin\frac{\pi y}{b} \\ w^{(2)} = w_0 \sin\frac{\pi x}{L} + w_b \sin\frac{n\pi x}{L} \sin\frac{\pi y}{b} \\ w^{(3)} = w^{(4)} = 0 , \end{cases} \tag{2a}$$

$$\begin{cases} u^{(1)} = -u_0 \frac{x}{L} + w_0 \frac{\pi}{L} \frac{b_1}{2} \cos\frac{\pi x}{L} + (u_{11} - u_{21} \cos\frac{2\pi y}{b}) \sin\frac{2n\pi x}{L} + u_3 \sin\frac{2\pi x}{L} \\ u^{(2)} = -u_0 \frac{x}{L} - w_0 \frac{\pi}{L} \frac{b_1}{2} \cos\frac{\pi x}{L} + (u_{12} - u_{22} \cos\frac{2\pi y}{b}) \sin\frac{2n\pi x}{L} + u_3 \sin\frac{2\pi x}{L} \\ u^{(3)} = u^{(4)} = -u_0 \frac{x}{L} + (y - \frac{b_1}{2}) w_0 \frac{\pi}{L} \cos\frac{\pi x}{L} + \frac{y}{b_1}[(u_{11}-u_{12})-(u_{21}-u_{22})]\sin\frac{2n\pi x}{L} \\ \qquad + (u_{12} - u_{22}) \sin\frac{2n\pi x}{L} + u_3 \sin\frac{2\pi x}{L} , \end{cases} \tag{2b}$$

$$\begin{cases} v^{(1)} = \frac{1}{b}(y - \frac{b}{2}) v_{11} + (v_{31} - v_{41} \cos\frac{2n\pi x}{L}) \sin\frac{2\pi y}{b} \\ v^{(2)} = \frac{1}{b}(y - \frac{b}{2}) v_{12} + (v_{32} - v_{42} \cos\frac{2n\pi x}{L}) \sin\frac{2\pi y}{b} \\ v^{(3)} = v^{(4)} = -w_0 \sin\frac{\pi x}{L} , \end{cases} \tag{2c}$$

where w_0, w_a, w_b, u_0, u_{11}, u_{21}, u_{12}, u_{22}, u_3, v_{11}, v_{31}, v_{41}, v_{12}, v_{32}, and v_{42} are the generalized coordinates.

The assumed initial eccentricities are expressed as follows:

$$\begin{cases} w_i^{(1)} = w_{0i} \sin\frac{\pi x}{L} - w_{1i} \sin\frac{n\pi x}{L} \sin\frac{\pi y}{b} \\ w_i^{(2)} = w_{0i} \sin\frac{\pi x}{L} + w_{1i} \sin\frac{n\pi x}{L} \sin\frac{\pi y}{b} \\ w_i^{(3)} = w_i^{(4)} = 0 , \end{cases} \tag{3a}$$

$$\begin{cases} u_i^{(1)} = w_{0i} \frac{\pi}{L} \frac{b_1}{2} \cos\frac{\pi x}{L} \\ u_i^{(2)} = -w_{0i} \frac{\pi}{L} \frac{b_1}{2} \cos\frac{\pi x}{L} \\ u_i^{(3)} = u_i^{(4)} = (y - \frac{b_1}{2}) w_{0i} \frac{\pi}{L} \cos\frac{\pi x}{L} , \end{cases} \tag{3b}$$

$$\begin{cases} v_i^{(1)} = v_i^{(2)} = 0 \\ v_i^{(3)} = v_i^{(4)} = -w_{0i} \sin \frac{\pi x}{L} \end{cases} . \tag{3c}$$

It should be pointed out that the above expressions for the assumed deflected shape and initial eccentricities apply equally well to the case of a panel formed by juxtaposition of rectangular tubes.

The conditions of continuity at the edges of the tube are satisfied, i.e.,

$$\begin{aligned}
w^{(1)}\Big|_{y=0} &= -v^{(3)}\Big|_{y=b_1} , & w^{(1)}\Big|_{y=b} &= -v^{(4)}\Big|_{y=b_1} \\
w^{(2)}\Big|_{y=0} &= -v^{(3)}\Big|_{y=0} , & w^{(2)}\Big|_{y=b} &= -v^{(4)}\Big|_{y=0} \\
u^{(1)}\Big|_{y=0} &= u^{(3)}\Big|_{y=b_1} , & u^{(1)}\Big|_{y=b} &= u^{(4)}\Big|_{y=b_1} \\
u^{(2)}\Big|_{y=0} &= u^{(3)}\Big|_{y=0} , & u^{(2)}\Big|_{y=b} &= u^{(4)}\Big|_{y=0}
\end{aligned} \tag{4}$$

When $w_0 = u_3 = 0$ and t_1 vanishes the problem reduces to plate action (see Appendix II). Then the assumed expressions for u, v, and w, given by Eqs. (2a), (2b), and (2c), are equivalent to those used by Mayers and Budiansky (8) in the elastic analysis of a simply supported square plate. In the latter analysis the authors assume that all edges are free to move in the plane of the plate and remain straight. This type of edge support is similar to that of the flange plates in the present problem. When edges A, B, C, and D shown in Fig. 1 are hinged, there is no restraint to the lateral displacement of the edges in the plane of the flanges. Even when the flanges are rigidly connected to the

side plates, only a small restraint would be expected to prevent the motion of the edges A, B, C, and D in the planes AB and CD, since the side plates AC and BD can be bent easily.

The general expressions for strain are given (15) by:

$$
\begin{aligned}
\epsilon_x &= \frac{\partial u}{\partial x} + \frac{1}{2}\left[\left(\frac{\partial u}{\partial x}\right)^2 + \left(\frac{\partial v}{\partial x}\right)^2 + \left(\frac{\partial w}{\partial x}\right)^2\right] \\
\epsilon_y &= \frac{\partial v}{\partial y} + \frac{1}{2}\left[\left(\frac{\partial u}{\partial y}\right)^2 + \left(\frac{\partial v}{\partial y}\right)^2 + \left(\frac{\partial w}{\partial y}\right)^2\right] \\
\epsilon_z &= \frac{\partial w}{\partial z} + \frac{1}{2}\left[\left(\frac{\partial u}{\partial z}\right)^2 + \left(\frac{\partial v}{\partial z}\right)^2 + \left(\frac{\partial w}{\partial z}\right)^2\right] \\
\gamma_{yz} &= \frac{\partial w}{\partial y} + \frac{\partial v}{\partial z} + \frac{\partial u}{\partial y}\frac{\partial u}{\partial z} + \frac{\partial v}{\partial y}\frac{\partial v}{\partial z} + \frac{\partial w}{\partial y}\frac{\partial w}{\partial z} \\
\gamma_{zx} &= \frac{\partial u}{\partial z} + \frac{\partial w}{\partial x} + \frac{\partial u}{\partial z}\frac{\partial u}{\partial x} + \frac{\partial v}{\partial z}\frac{\partial v}{\partial x} + \frac{\partial w}{\partial z}\frac{\partial w}{\partial x} \\
\gamma_{xy} &= \frac{\partial v}{\partial x} + \frac{\partial u}{\partial y} + \frac{\partial u}{\partial x}\frac{\partial u}{\partial y} + \frac{\partial v}{\partial x}\frac{\partial v}{\partial y} + \frac{\partial w}{\partial x}\frac{\partial w}{\partial y}
\end{aligned}
\tag{5}
$$

The above expressions are simplified, in the theory of large deflections of medium-thick plates (3), by taking $\epsilon_z = \gamma_{yz} = \gamma_{zx} = 0$; the terms $\left(\frac{\partial u}{\partial x}\right)^2$, $\left(\frac{\partial u}{\partial y}\right)^2$, $\left(\frac{\partial v}{\partial x}\right)^2$, $\left(\frac{\partial v}{\partial y}\right)^2$, $\frac{\partial u}{\partial x}\frac{\partial u}{\partial y}$, and $\frac{\partial v}{\partial x}\frac{\partial v}{\partial y}$ are neglected since they are small compared to $\left(\frac{\partial w}{\partial x}\right)^2$, $\left(\frac{\partial w}{\partial y}\right)^2$ and $\frac{\partial w}{\partial x}\frac{\partial w}{\partial y}$. These simplifications are valid for the flange plates AB and CD; however for the side plates the terms $\left(\frac{\partial v}{\partial x}\right)^2$ and $\left(\frac{\partial v}{\partial y}\right)^2$ are significant since they contain the w_0 coordinate.

If a plate has an initially curved surface described by the functions w_i, u_i, and v_i, the middle surface strains given by Eqs. 5 must be revised as follows (6),

$$
\begin{aligned}
\epsilon_x &= \frac{\partial u}{\partial x} - \frac{\partial u_i}{\partial x} + \frac{1}{2}\left(\frac{\partial w}{\partial x}\right)^2 - \frac{1}{2}\left(\frac{\partial w_i}{\partial x}\right)^2 \\
\epsilon_y &= \frac{\partial v}{\partial y} - \frac{\partial v_i}{\partial y} + \frac{1}{2}\left(\frac{\partial w}{\partial y}\right)^2 - \frac{1}{2}\left(\frac{\partial w_i}{\partial y}\right)^2
\end{aligned}
\tag{6}
$$

$$\gamma_{xy} = \frac{\partial v}{\partial x} - \frac{\partial v_i}{\partial x} + \frac{\partial u}{\partial y} - \frac{\partial u_i}{\partial y} + \frac{\partial w}{\partial x}\frac{\partial w}{\partial y} - \frac{\partial w_i}{\partial x}\frac{\partial w_i}{\partial y} \quad . \qquad (6) \text{ cont'd.}$$

The above equations apply to the flange plates. The strains for the side plates are obtained by replacing in the above expressions the w's by the v's since the latter represent the significant displacements and w = 0 for those plates. Hence, for the side plates,

$$\begin{aligned}
\epsilon_x &= \frac{\partial u}{\partial x} - \frac{\partial u_i}{\partial x} + \frac{1}{2}\left(\frac{\partial v}{\partial x}\right)^2 - \frac{1}{2}\left(\frac{\partial v_i}{\partial x}\right)^2 \\
\epsilon_y &= \frac{\partial v}{\partial y} - \frac{\partial v_i}{\partial y} + \frac{1}{2}\left(\frac{\partial v}{\partial y}\right)^2 - \frac{1}{2}\left(\frac{\partial v_i}{\partial x}\right)^2 \qquad (7) \\
\gamma_{xy} &= \frac{\partial v}{\partial x} - \frac{\partial v_i}{\partial x} + \frac{\partial u}{\partial y} - \frac{\partial u_i}{\partial y} + \frac{\partial v}{\partial x}\frac{\partial v}{\partial y} - \frac{\partial v_i}{\partial x}\frac{\partial v_i}{\partial y} \quad .
\end{aligned}$$

The strain energy of the deflected column consists of two parts: the strain energy V_S due to membrane stresses and the strain energy V_B due to bending. V_S is given (3) by,

$$V_S = \frac{Et}{2}\iint \left(\epsilon_x^2 + \epsilon_y^2 + \frac{1}{2}\gamma_{xy}^2\right) dxdy \qquad (8)$$

for Poisson's ratio equal to zero.

The strain energy due to bending V_B, in the case of a straight plate, is given (3) by,

$$V_B = \frac{D}{2}\iint \left\{\left(\frac{\partial^2 w}{\partial x^2} + \frac{\partial^2 w}{\partial y^2}\right)^2 - 2\left[\frac{\partial^2 w}{\partial x^2}\frac{\partial^2 w}{\partial y^2} - \left(\frac{\partial^2 w}{\partial x \partial y}\right)^2\right]\right\} dxdy \qquad (9)$$

also assuming that $\nu = 0$.

For initially eccentric plates (6), the curvatures $\frac{\partial^2 w}{\partial x^2}$, $\frac{\partial^2 w}{\partial y^2}$, and $\frac{\partial^2 w}{\partial x \partial y}$ are replaced by the changes in curvature $\frac{\partial^2}{\partial x^2}(w-w_i)$, $\frac{\partial^2}{\partial y^2}(w-w_i)$, and

$\frac{\partial^2}{\partial x \partial y}(w-w_i)$. Then

$$V_B = \frac{D}{2}\iint (T_a^2 - 2T_b + 2T_c^2)\, dxdy \tag{10}$$

where,

$$\begin{aligned} T_a &= \frac{\partial^2}{\partial x^2}(w-w_i) + \frac{\partial^2}{\partial y^2}(w-w_i) \\ T_b &= \frac{\partial^2}{\partial x^2}(w-w_i)\,\frac{\partial^2}{\partial y^2}(w-w_i) \\ T_c &= \frac{\partial^2}{\partial x \partial y}(w-w_i) \end{aligned} \tag{11}$$

The potential energy V_P is the product of the applied load by the axial shortening of the column, i.e.,

$$V_P = -2\,\sigma\,(bt + b_1 t_1)\,u_0 . \tag{12}$$

According to the Rayleigh-Ritz method, the generalized coordinates are determined by minimizing the total energy of the system. If g represents a generalized coordinate, the condition for a stationary energy is

$$\frac{\partial V_T}{\partial g} = 0 \tag{13}$$

and $V_T = V_S + V_B + V_P$, where V_S and V_B are extended to all the component plates.

It is easier to compute $\frac{\partial V_T}{\partial g}$ directly without actually computing V_T; this is so because of the orthogonality of the trigonometric terms. Consequently Eq. 13 can be replaced by,

$$\begin{aligned} \frac{\partial V_T}{\partial g} = \sum_{j=1}^{j=4} \Bigg\{ & Et^{(j)} \int_0^L \int_0^{b^{(j)}} [\epsilon_x^{(j)} \frac{\partial \epsilon_x^{(j)}}{\partial g} + \epsilon_y^{(j)} \frac{\partial \epsilon_y^{(j)}}{\partial g} + \frac{1}{2}\gamma_{xy}^{(j)} \frac{\partial \gamma_{xy}^{(j)}}{\partial g}]\, dxdy \\ & + D^{(j)} \int_0^L \int_0^{b^{(j)}} [T_a^{(j)} \frac{\partial T_a^{(j)}}{\partial g} - \frac{\partial T_b^{(j)}}{\partial g} + 2T_c^{(j)} \frac{\partial T_c^{(j)}}{\partial g}]\, dxdy \Bigg\} + \frac{\partial V_P}{\partial g} = 0 \end{aligned} \tag{14}$$

where

$$t^{(1)} = t^{(2)} = t \quad , \quad t^{(3)} = t^{(4)} = t_1$$

$$b^{(1)} = b^{(2)} = b \quad , \quad b^{(3)} = b^{(4)} = b_1$$

$$D^{(1)} = D^{(2)} = Et^3/12 \quad , \quad D^{(3)} = D^{(4)} = Et_1^3/12 \ .$$

In order to compute the terms of Eq. (14) for the fifteen generalized coordinates used in the present analysis it is convenient to:

(a) Compute the values of $\epsilon_x^{(j)}$, $\epsilon_y^{(j)}$, $\gamma_{xy}^{(j)}$, $T_a^{(j)}$, $T_b^{(j)}$, and $T_c^{(j)}$ for the four sides of the tube, by substituting the corresponding assumed deflections $u^{(j)}$, $v^{(j)}$, $w^{(j)}$, and the initial eccentricities $u_i^{(j)}$, $v_i^{(j)}$, $w_i^{(j)}$ as given by Eqs. (2a), (2b), (2c), (3a), (3b), (3c), into expressions (6) or (7) and (11).

(b) Compute the derivatives $\frac{\partial \epsilon_x^{(j)}}{\partial g}$, $\frac{\partial \epsilon_y^{(j)}}{\partial g}$, $\frac{\partial \gamma_{xy}^{(j)}}{\partial g}$, $\frac{\partial T_a^{(j)}}{\partial g}$, $\frac{\partial T_b^{(j)}}{\partial g}$, and $\frac{\partial T_c^{(j)}}{\partial g}$ and then evaluate the double integrals of Eq. (14).

Following this computational scheme, one obtains a system of 15 nonlinear simultaneous algebraic equations corresponding to the 15 generalized coordinates. It is assumed in step (b) that the flanges buckle in a square pattern. Furthermore in the process of integration, n is assumed to be even and larger than 4. According to a more rigorous solution by Stein (9), the assumption that the plates buckle in square panels is only valid in the early post-buckling range. Also, the assumed deflected shape for the component plates are approximate and known to be valid only in the beginning of the post-buckling stage. Consequently the equations derived in the present analysis are only expected to yield significant results when the critical load of the plate is not greatly exceeded.

Setting

$$I_1 = \left(\frac{w_a^2}{b^2} - \frac{w_{1i}^2}{b^2}\right)\frac{\pi}{16}, \qquad I_2 = \left(\frac{w_b^2}{b^2} - \frac{w_{1i}^2}{b^2}\right)\frac{\pi}{16}$$

$$I_3 = \left(\frac{w_b^2}{b^2} - \frac{w_a^2}{b^2}\right)\frac{\pi}{8}\,\frac{b_1}{b}\,\frac{2-4n^2}{n(1-4n^2)}$$

$$I_4 = \left[\frac{w_0}{L}\left(\frac{w_a^2}{b^2} + \frac{w_b^2}{b^2}\right) - \frac{w_{0i}}{L}\,\frac{w_{1i}}{b}\left(\frac{w_a}{b} + \frac{w_b}{b}\right)\right]\frac{3\pi^2}{16}$$

$$H_1 = \left(\frac{w_0}{L} - \frac{w_{0i}}{L}\right)\left(\frac{b_1}{b} + \frac{1}{3}\,\frac{b_1^2}{b^2}\,\frac{t_1}{t}\right)\frac{2}{n(4n^2-1)}$$

$$H_2 = \left(\frac{w_0}{L} - \frac{w_{0i}}{L}\right)\frac{b_1^2}{b^2}\,\frac{t_1}{t}\,\frac{2}{3n(4n^2-1)}$$

$$H_3 = \left(\frac{w_0}{L} - \frac{w_{0i}}{L}\right)\left(\frac{b_1^2}{b^2} + \frac{1}{3}\,\frac{b_1^3}{b^3}\,\frac{t_1}{t} + \frac{1}{3}\,\frac{t^2}{b^2}\right)\frac{\pi^2}{4}\,\frac{1}{n^2}$$

$$H_4 = \left(\frac{w_0}{L} - \frac{w_{0i}}{L}\right)\frac{\pi}{4}\,\frac{b_1}{b}\,\frac{2-4n^2}{n(1-4n^2)}$$

$$H_5 = \left(\frac{w_a}{b} - \frac{w_{1i}}{b}\right)\frac{\pi^2}{12}\,\frac{t^2}{b^2} \qquad (15)$$

$$H_6 = \left(\frac{w_b}{b} - \frac{w_{1i}}{b}\right)\frac{\pi^2}{12}\,\frac{t^2}{b^2}$$

$$J_1 = \left[\left(\frac{u_{11}}{b} - \frac{u_{12}}{b}\right) - \left(\frac{u_{21}}{b} - \frac{u_{22}}{b}\right)\right]\left(\frac{4}{3}\,\frac{b_1}{b} + \frac{1}{2\pi^2}\,\frac{b}{b_1}\right)\frac{t_1}{t}$$

$$J_2 = \left[\left(\frac{u_{11}}{b} - \frac{u_{12}}{b}\right) - \left(\frac{u_{21}}{b} - \frac{u_{22}}{b}\right)\right]\left(\frac{2}{3}\,\frac{b_1}{b} - \frac{1}{2\pi^2}\,\frac{b}{b_1}\right)\frac{t_1}{t}$$

$$J_3 = 2\left(\frac{u_{12}}{b} - \frac{u_{22}}{b}\right)\frac{b_1}{b}\,\frac{t_1}{t}$$

$$J_4 = \left(\frac{u_{12}}{b} - \frac{u_{11}}{b}\right)\frac{b_1}{b}\,\frac{2}{n(1-4n^2)}$$

$$J_5 = \left[\left(\frac{u_{11}}{b} - \frac{u_{12}}{b}\right) - \left(\frac{u_{21}}{b} - \frac{u_{22}}{b}\right)\right]\frac{b_1^2}{b^2}\,\frac{t_1}{t}\,\frac{2}{3n(1-4n^2)}$$

$$J_6 = \frac{w_a}{b}\left(\frac{u_{11}}{b} + \frac{u_{21}}{b} + \frac{v_{41}}{b} + \frac{v_{31}}{b} + \frac{1}{\pi}\frac{v_{11}}{b}\right)\frac{\pi}{4}$$

$$J_7 = \frac{w_b}{b}\left(\frac{u_{12}}{b} + \frac{u_{22}}{b} + \frac{v_{42}}{b} + \frac{v_{32}}{b} + \frac{1}{\pi}\frac{v_{12}}{b}\right)\frac{\pi}{4}$$

$$K_1 = \left(\frac{w_0^2}{L^2} - \frac{w_{0i}^2}{L^2}\right)\frac{\pi}{8} \qquad (15) \text{ cont'd.}$$

$$K_2 = \frac{w_0}{L}\left(\frac{w_0}{L}\frac{w_a}{b} - \frac{w_{0i}}{L}\frac{w_{1i}}{b}\right)\frac{3\pi^2}{16}$$

$$K_3 = \frac{w_0}{L}\left(\frac{w_0}{L}\frac{w_b}{b} - \frac{w_{0i}}{L}\frac{w_{1i}}{b}\right)\frac{3\pi^2}{16}$$

the system of nonlinear simultaneous algebraic equations can be written as follows. The parameter between the brackets [ ], at the left of each equation, indicates the generalized coordinate with respect to which the total energy was differentiated.

$$[v_{11}] \qquad \frac{v_{11}}{b} + 2\pi I_1 = 0 \qquad (16)$$

$$[v_{12}] \qquad \frac{v_{12}}{b} + 2\pi I_2 = 0 \qquad (17)$$

$$[v_{31}] \qquad \frac{v_{31}}{b} + I_1 = 0 \qquad (18)$$

$$[v_{32}] \qquad \frac{v_{32}}{b} + I_2 = 0 \qquad (19)$$

$$[v_{41}] \qquad \frac{3}{2}\frac{v_{41}}{b} + \frac{1}{2}\frac{u_{21}}{b} + 2I_1 = 0 \qquad (20)$$

$$[v_{42}] \qquad \frac{3}{2}\frac{v_{42}}{b} + \frac{1}{2}\frac{u_{22}}{b} + 2I_2 = 0 \qquad (21)$$

$$[u_{11}] \qquad H_1 + \frac{2u_{11}}{b} + 2I_1 + J_1 + J_3 = 0 \qquad (22)$$

$$[u_{12}] \qquad -H_1 + \frac{2u_{12}}{b} + 2I_2 + J_2 + J_3 = 0 \tag{23}$$

$$[u_{21}] \qquad \frac{3}{2}\frac{u_{21}}{b} + \frac{1}{2}\frac{v_{41}}{b} + 2I_1 - H_2 - J_1 - J_3 = 0 \tag{24}$$

$$[u_{22}] \qquad -\frac{3}{2}\frac{u_{22}}{b} + \frac{1}{2}\frac{v_{42}}{b} + 2I_2 + H_2 - J_2 - J_3 = 0 \tag{25}$$

$$[u_0] \qquad \frac{u_0}{L} - 2\pi K_1 - \pi(I_1 + I_2)\left(1 + \frac{b_1}{b}\frac{t_1}{t}\right)^{-1} - \frac{\mathfrak{C}}{E} = 0 \tag{26}$$

$$[u_3] \qquad \frac{u_3}{L} + K_1 = 0 \tag{27}$$

$$[w_0] \qquad H_3 + J_4 + I_3 + \frac{w_0}{L}\left(1 + \frac{b_1}{b}\frac{t_1}{t}\right)\left(\frac{\pi u_3}{L} - \frac{u_0}{L} + 3\pi K_1\right) + \frac{\pi w_0}{L}(I_1 + I_2) + I_4 - J_5 = 0 \tag{28}$$

$$[w_a] \qquad -\frac{1}{4}\frac{u_0}{L}\frac{w_a}{b} - H_4 + J_6 + \frac{\pi}{2}\frac{w_a}{b}K_1 + K_2 + \frac{5}{2}\pi\frac{w_a}{b}I_1 + H_5 = 0 \tag{29}$$

$$[w_b] \qquad -\frac{1}{4}\frac{u_0}{L}\frac{w_b}{b} + H_4 + J_7 + \frac{\pi}{2}\frac{w_b}{b}K_1 + K_3 + \frac{5}{2}\pi\frac{w_b}{b}I_2 + H_6 = 0 \tag{30}$$

It should be pointed out that the above system of equations represent the condition for stationary energy, i.e. minimum or maximum corresponding to positions of stable or unstable equilibrium respectively. In order to determine the type of equilibrium corresponding to a given solution of the above set of equations it would be necessary to examine the second variation of the total energy. This, however, involves extremely lengthy computations. The stability in the present analysis is investigated by studying the results obtained for different eccentricities and by comparison with plate and column action separately.

III NUMERICAL SOLUTION

8. Method of Solution

Newton's method is used to solve the system of nonlinear algebraic simultaneous equations. The selection of this method of solution has been based on the accessibility of a high-speed digital computer, for which standard subroutines to solve systems of linear equations are available. The detailed description of Newton's method may be found in various texts on numerical methods (16) and is summarized as follows. Given a system of n equations with n unknowns,

$$
\begin{aligned}
&F_1\,(x_1, x_2, \ldots, x_i, \ldots, x_n) = 0 \\
&F_2\,(x_1, x_2, \ldots, x_i, \ldots, x_n) = 0 \\
&\;\;\vdots \\
&F_j\,(x_1, x_2, \ldots, x_i, \ldots, x_n) = 0 \\
&\;\;\vdots \\
&F_n\,(x_1, x_2, \ldots, x_i, \ldots, x_n) = 0 \quad ,
\end{aligned}
\tag{31}
$$

it is possible to expand any of the functions, F_j's, by Taylor's series. Hence,

$$
\begin{aligned}
&F_j\,(x_1 + \Delta x_1, x_2 + \Delta x_2, \ldots, x_i + \Delta x_i, \ldots, x_n + \Delta x_n) = \\
&F_j\,(x_1, x_2, \ldots, x_i, \ldots, x_n) + \Delta x_1 \frac{\partial F_j}{\partial x_1} + \Delta x_2 \frac{\partial F_j}{\partial x_2} + \ldots + \Delta x_i \frac{\partial F_j}{\partial x_i} + \ldots + \\
&\qquad + \Delta x_n \frac{\partial F_j}{\partial x_n} + \Delta^2 \,,
\end{aligned}
\tag{32}
$$

where Δ^2 represents second and higher order terms which are neglected when the Δx_i's are small. By using this type of expansion, Eqs. (31) transform into the following system of equations which are linear in terms of the Δx_i's,

$$\begin{vmatrix} F_1 \\ F_2 \\ \cdot \\ \cdot \\ \cdot \\ F_j \\ \cdot \\ \cdot \\ \cdot \\ F_n \end{vmatrix} + \begin{vmatrix} \frac{\partial F_1}{\partial x_1} & \frac{\partial F_1}{\partial x_2} & \cdots & \frac{\partial F_1}{\partial x_i} & \cdots & \frac{\partial F_1}{\partial x_n} \\ \frac{\partial F_2}{\partial x_1} & \frac{\partial F_2}{\partial x_2} & \cdots & \frac{\partial F_2}{\partial x_i} & \cdots & \frac{\partial F_2}{\partial x_n} \\ \cdot & \cdot & & \cdot & & \cdot \\ \cdot & \cdot & & \cdot & & \cdot \\ \cdot & \cdot & & \cdot & & \cdot \\ \frac{\partial F_j}{\partial x_1} & \frac{\partial F_j}{\partial x_2} & \cdots & \frac{\partial F_j}{\partial x_i} & \cdots & \frac{\partial F_j}{\partial x_n} \\ \cdot & \cdot & & \cdot & & \cdot \\ \cdot & \cdot & & \cdot & & \cdot \\ \cdot & \cdot & & \cdot & & \cdot \\ \frac{\partial F_n}{\partial x_1} & \frac{\partial F_n}{\partial x_2} & \cdots & \frac{\partial F_n}{\partial x_i} & \cdots & \frac{\partial F_n}{\partial x_n} \end{vmatrix} \cdot \begin{vmatrix} \Delta x_1 \\ \Delta x_2 \\ \cdot \\ \cdot \\ \cdot \\ \Delta x_i \\ \cdot \\ \cdot \\ \cdot \\ \Delta x_n \end{vmatrix} = 0 \qquad (33)$$

The numerical solution of the above system of equations can proceed in an iterative fashion by applying the following steps:

(a) Assume a set of initial values $x_1, x_2, \ldots, x_i, \ldots, x_n$.

(b) Compute the coefficients $\frac{\partial F_j}{\partial x_i}$ and F_j of Eqs. (33); solve the system of linear equation thus determining $\Delta x_1, \Delta x_2, \ldots, \Delta x_i, \ldots, \Delta x_n$.

(c) If the Δx_i's are not small, correct the previously assumed set of x_i's by adding algebraically the corresponding values of the Δx_i's.

(d) Repeat steps (b) and (c) using the corrected set of x_i's until all Δx_i's become small.

This method has proved to converge satisfactorily for a large class of nonlinear equations. Crandall (17) points out that ... "the process may not pull in, or it may converge toward a solution which is physically uninteresting although mathematically correct. Several trials may be necessary to locate the neighbor-

hood of the desired solution." This possibility was investigated in the present solution and will be discussed later in this chapter.

In the present problem the unknowns $x_1, x_2, \ldots x_i \ldots x_n$ stand for the dimensionless parameters, $\frac{w_0}{L}, \frac{w_a}{b}, \frac{w_b}{b} \ldots$ etc. representing the generalized coordinates.

9. Programming

A computer program has been prepared for the solution of the system of Eqs. (16) through (30), using the iterative procedure described in the previous section. This program is coded for use in the ILLIAC, the high-speed digital computer at the University of Illinois.

In order to reduce the time of computation it is convenient to eliminate the variables $v_{11}, v_{12}, v_{31}, v_{32}$, and u_3 by substituting Eqs. (16), (17), (18), (19), and (27) into the remaining equations of the system. This reduces the system to ten equations with ten unknowns. Further reduction of the number of variables will be examined later.

The coefficients $\frac{\partial F_j}{\partial x_i}$ and F_j for the system of ten equations have been computed by hand and properly scaled as to comply with the requirements of a standard library subroutine to solve linear equations. Fig. 3 depicts the simplified flow diagram upon which the program is based. The program starts by reading from a data tape the constants defining the geometry of the column and the initial eccentricities. These constants are expressed in a dimensionless form by the ratios b/L, t/b, b_1/b, t_1/t, w_{0i}/L, w_{1i}/b, modified by suitable scaling factors.

Next step is taken by computing the constants that appear in the coefficients $\frac{\partial F_j}{\partial x_i}$ and F_j containing terms that depend only on the geometry of the tube. Also, the Euler stress

$$\sigma_E = \pi^2 \frac{EI_t}{AL^2}$$

is determined and a fraction of its value is taken as applied stress increment($\Delta\sigma$). This step is followed by setting the proper initial values of the unknowns when the load is equal to zero. They are,

$$u_0 = u_3 = u_{11} = u_{12} = u_{21} = u_{22} = v_{11} = v_{12} = v_{31} = v_{32} = v_{41} = v_{42} = 0$$
$$w_0 = w_{01}, \quad w_a = w_b = w_{11} \quad . \tag{34}$$

With the above value of the unknowns the coefficients $\frac{\partial F_j}{\partial x_i}$ and F_j are computed and the system of linear equations is solved, thereby determining the Δx_i's. A test is then performed to check if all Δx_i's are small. If all $|\Delta x_i|$'s are smaller than α the computer is ordered to print the values of the x_i's utilized in the last cycle of computation. This is usually the case when $\sigma = 0$ since the initial values given by Eqs. (34) are exact. This step is followed by adding an increment to the load and recomputing the coefficients $\frac{\partial F_j}{\partial x_i}$ and F_j.

If any of the $|\Delta x_i|$'s is greater than α the operation

$$x_i' = x_i + \Delta x_i$$

is performed and the coefficients $\frac{\partial F_j}{\partial x_i}$ and F_j re-evaluated; the computation then proceeds according to the iterative procedure described in the previous section. The values $\alpha = 10^{-7}$ and $\Delta\sigma = \frac{1}{40}\sigma_E$ have been chosen by trials so as to reduce, as much as possible, the total time of computation.

Besides printing the values of the unknown x_i's, the following quantities are also printed:

(a) value of the corresponding applied stress σ and its percentage of σ_E,

(b) number of cycles necessary for convergence,

(c) strains at critical points of the cross section.

The computation is interrupted by means of an end test when w_0/L becomes excessively large thus invalidating the assumptions made in the small deflection

theory of columns. Furthermore, special stops are provided in the case of slow convergence or divergence of the iterative procedure and also in the case of overflow.

A desirable feature that has been added to the main program is the capability of starting the computations at any level of load, with the initial trial values of the variables being given in a data tape. Modified programs have been prepared also for column and plate action separately (see Appendices I and II). In these cases the initial values of the coordinates to be eliminated are set equal to zero and the corresponding equations (16) through (30) replaced by equations of the type $\Delta x_i = 0$.

A modified program has been prepared also to solve the system of nonlinear equations considering σ/E as one of the unknown x_i's, instead of w_0/L. The ratio w_0/L is then increased by steps instead of the applied stress. Such a program enables one to verify the possibility of a maximum in the σ/E vs. w_0/L diagram, which might not be detected in the original program.

The code-checking has been accomplished by reading into the computer assumed values for the x_i's. The coefficients $\frac{\partial F_j}{\partial x_i}$ and F_j are then computed, printed and checked with the results obtained by performing the same operations with a desk calculator. The stability of the numerical computation has been verified by starting with different initial sets of values for the unknowns and comparing the final results after enough iterative cycles had taken place.

The total time of computation for the main program, starting from zero load, is approximately twenty minutes. The approximate number of cycles for convergence is three when the plates are in the pre-buckling range and fifteen when they are in the post-buckling range.

Various trials with different values of the goemetry and initial eccentricities have shown that the equations can be further simplified when the quan-

tities H_1, H_2, J_1, J_2, J_3 are small compared to the other terms in Eqs. (22), (23), (24), and (25). This has proved to be true for the geometries and eccentricities presented in the next chapter. In this case Eqs. (20), (22), (24), and (21), (23), (25) yield,

$$u_{11} = u_{21} = v_{41} = - I_1 b$$

$$u_{12} = u_{22} = v_{42} = - I_2 b \quad .$$

This reduces the system to four equations and four unknowns: w_0/L, w_a/b, w_b/b, u_0/L. A similar program has been prepared for this case and the computation time reduces to seven minutes.

In order to determine the validity of the above simplification the representative results for each set of solutions presented herein have been checked against those obtained by utilizing ten variables.

IV PRESENTATION OF RESULTS

10. General Remarks

The program described in the previous section has been utilized to solve numerically the system of equations derived in Chapter II, for different values of the geometry and initial eccentricities. The results are presented in the form of diagrams expressing the variation of various displacements of the structure with the applied load.

Four different values of L/b have been considered, and the following parameters studied:

(a) initial eccentricity of the column and plate,

(b) ratio of the plate critical stress to the Euler stress for the column, i.e. $\sigma_{cr}^{pl}/\sigma_E$,

(c) ratio of the inertia of the flanges to the total inertia of the cross section, i.e. I_f/I_t .

The effect of each of the above parameters has been investigated by varying its value while the others are kept unchanged. The significant results are presented in Figs. 6 through 17.

In Figs. 6, 10, 13, and 17, w_0/L is plotted versus the ratio σ/σ_E, for columns with L/b ratios of 20, 30, 50, and 70 respectively. These diagrams show the effect of the initial eccentricity of the column, w_{0i}/L, when the other variables are kept constant. The t/b ratios have been chosen so that $\sigma_{cr}^{pl}/\sigma_E$ equals 0.8; t_1/t and b_1/b are constants and equal to 1.5 and 1.0 respectively; therefore the web plates are not expected to buckle during the loading of the column. The dashed lines in the above mentioned figures are branches of hyperbolas given by the well known expression,

$$\frac{w_0}{L} = \frac{w_{0i}}{L} \frac{1}{1 - \sigma/\sigma_E} \tag{35}$$

which represents the center deflection of an initially eccentric column, with a shape of a half sine wave, loaded at the stress level σ. These dashed lines are referred to as column action curves since they represent the behavior of the column if the plates did not buckle. Points are marked on the curves of Figs. 6, 10, 13, and 17 to indicate various strain levels for the surface point where the maximum strain is more likely to occur: the buckle crest, in the compression flange, close to the center of the column. The strain levels indicate how much a column of a given material can deflect laterally without plastic strains. As it will be seen later these strain levels are approximate and are only used to give an idea of the range of applicability of the present elastic analysis. For example, when the column material is structural grade steel, with a limiting elastic strain of approximately 0.001, the present study applies to the case presented in Fig. 17; however it does not apply to the case presented in Fig. 6 since higher values of maximum strain occur in the column before plate buckling takes place.

Fig. 7 depicts the variation of the displacements w_a and w_b with the applied stress σ, for the same geometry and initial eccentricities shown in the case of Fig. 6. The curves expressing the variation of the displacements w_a and w_b with the applied load, for columns with other L/b ratios, show the same general trend.

Fig. 8 shows the effect of different plate eccentricities on the w_0/L, σ/σ_E diagram for a column with an L/b ratio of 20. Corresponding w_a/b and w_b/b, σ/σ_E curves are presented in Fig. 9. The same general characteristics have been observed for columns with other L/b ratios.

Fig. 14 shows the effect of the ratio $\sigma_{cr}^{pl}/\sigma_E$ on the w_0/L, σ/σ_E curves for an L/b ratio of 50. The values of t/b have been chosen so as to give ratios $\sigma_{cr}^{pl}/\sigma_E$ equal to 0.7, 0.8, and 0.9. Fig. 15 depicts the corresponding

w_a/b and w_b/b, σ/σ_E diagram. Curves for L/b ratios of 20, 30, and 70 exhibit the same characteristics and are not reported.

Middle surface and surface strains at critical points of the cross section are presented in Fig. 16 for a column with an L/b of 50. The strain distributions for columns with other L/b ratios are similar to that of Fig. 16 and are not presented herein. As in the case of plate action (see Appendix II), the strains may entail appreciable errors. The main purpose of Fig. 16 is to give an indication of the strain magnitude at various points of the middle section of the column.

The effect of the ratio I_f/I_t is shown in Figs. 11 and 12 for an L/b ratio of 30. Similar curves have been obtained for other L/b ratios.

11. Limitations

The solution of the nonlinear equations derived in Chapter II presented some difficulties in the case of certain values of the parameters representing the geometry and initial eccentricities. An attempt to increase the ratio I_f/I_t above 0.9 or to decrease the ratio $\sigma_{cr}^{pl}/\sigma_E$ below 0.6, resulted in maximum applied stresses much higher than σ_E. A similar behavior has been observed in the case of columns exhibiting large plate eccentricities. These difficulties seem to stem from the same source: the inadequacy of the assumed deflected shape for the flange plates when fairly large deflections are involved. It has been pointed out previously that the assumed deflected shape would only be expected to yield significant results in the early post-buckling behavior of the plates, when the displacements are not excessively large. It has also been mentioned that according to Stein (9), a change in the buckling pattern may occur in the post-buckling range. Stein investigated the behavior of an infinitely long strip, which resembles the flange plates in the present analysis, and

pointed out that after the strip buckles in a square pattern there is a continual increase in the number of buckle waves with increasing load.

In order to improve the present analysis, to take into account larger deflections of the component plates, each or both of the alternatives indicated below could be followed:

(a) Add another term to the w displacement expression for the flange plates, similar to that suggested by Marguerre (2) in the post-buckling analysis of very thin plates.

(b) Consider as unknowns the number of buckle waves in each flange and determine, for each load increment, the combination of their values that gives a minimum of total energy.

Both alternatives would increase considerably the labor involved in the computations.

Another type of difficulty encountered in the numerical solution of the nonlinear equations is concerned with the value of the initial plate eccentricity. It has been found that for very small plate eccentricities, the computation proceeds normally up to the point where plate buckling occurs. Then the convergence becomes very slow or, in certain cases, the iterative procedure diverges. This may be explained by the fact that round-off errors become significant when small quantities are involved in the computations.

12. Analysis of Results

Since the concepts of critical load and maximum load will be used frequently in this section, it is desirable to review them briefly. The critical load of a perfectly straight column is the load at which the column starts to deflect laterally. In the present analysis this load can be inferred by analyzing the behavior of the column when the initial eccentricity tends to zero.

After a straight column starts to deflect it may or may not carry additional load, depending on the stress-strain characteristics of the column material. The maximum load is the greatest load to which the column can be subjected.

According to the small deflection theory, the maximum load equals the critical load when the column material is linearly elastic. Shanley (2) has shown that the critical load of columns made of materials exhibiting a nonlinear stress-strain diagram, corresponds to the tangent modulus load. For such columns the maximum load depends on the shape of the stress-strain diagram of the column material (10).

In this analysis the maximum load cannot be determined exactly since the load applied to the column increases little, but steadily, after the plates have buckled (Figs. 6, 10, 13, and 17), and the theory does not apply when large deflections are involved.

Figs. 6, 8, 10, 11, 13, 14, and 17 show that the critical load of the column is equal to the critical load of the flange plates when the plate eccentricity tends to zero. Even when the ratio I_f/I_t is small, such as in one of the cases of Fig. 11 where it equals .27, the lateral deflections start to differ from the column action at the plate critical load. This is in agreement with Shanley's theory which predicts that the critical load of a column is the tangent modulus load.

Figs. 6, 10, 13, and 17 indicate that for the same initial plate eccentricity, the difference between curves representing column action (dashed lines) and combined action (solid lines) decreases for increasing w_{01}/L. Furthermore, after the plates buckle, there is little increase in the load carrying capacity in the case of columns exhibiting small initial imperfections; this small increase in load is accompanied by fairly large increase in lateral deflection.

Fig. 7 depicts clearly the "strain reversal" in the flanges after the critical load of the plates is reached. The "strain reversal" is characterized

by a sudden reduction in the value of w_b and a continuous increase in w_a. This again agrees with Shanley's theory: the strain reversal takes place at the tangent modulus load. This fact is further evidenced by the strain diagrams presented in Fig. 16. It is interesting to note that for columns exhibiting larger eccentricities, such as the curve for $w_{01}/L = 0.0005$ in Fig. 7, the local buckling of the tension flange might not occur at all.

Figs. 8 and 9 show the importance of the initial plate eccentricity in the behavior of the column, after the side plates buckle. The critical load of a column with plates exhibiting larger initial eccentricity is lower than the critical load for the component plates. The maximum load, however, depends largely on the initial plate eccentricity: the greater the eccentricity of the plate, the higher is the maximum load that can be applied to the column. This conclusion may be justified by studying in detail the curves presented in Fig. 5 (see Appendix II), which in previous remarks was shown to represent the equivalent stress-strain diagram for the flanges of the thin-walled rectangular tube. It is shown in Fig. 5 that there is a gradual change in the slope of the load-displacement curve, in the case of plates exhibiting larger initial eccentricity. When the initial plate eccentricity tends to zero, there is a marked change in the slope at the vicinity of the plate buckling load. Duberg and Wilder (10) have pointed out that ... "for columns in which the material stress-strain curves depart gradually from the initial slope as is characteristic of stainless steels, the maximum column load may be significantly above the tangent modulus load. If the departure from the elastic curve is more abrupt such as in high strength aluminum or magnesium alloys, the maximum load is only slightly above the tangent modulus load." Consequently, the curves presented in Fig. 5 when regarded as equivalent stress-strain diagrams justify the conclusion drawn previously about the effect of initial plate eccentricity on the behavior of the column. The importance of the local eccentricities is not surprising since it

has shown to be a critical factor in tests and theoretical analysis of various types of thin shells (3).

It can be concluded from Figs. 14 and 15 that although the critical load of the column always corresponds to the buckling load of the component plates, the ratio $\sigma_{max}/\sigma_{cr}^{pl}$ decreases when the ratio $\sigma_{cr}^{pl}/\sigma_E$ increases. Finally, Figs. 11 and 12 show that the maximum applied stress increases for a decreasing I_f/I_t ratio.

V CONCLUSIONS

13. Summary

If one bears in mind the limitations mentioned in paragraph 11, the important conclusions derived in the previous chapter may be summarized as follows:

(1) The critical load of a column is equal to the buckling load of the component plates when the plate eccentricity tends to zero; for larger plate eccentricities the critical load of the column is lower than that of plate buckling.

(2) The maximum load to which the column may be subjected depends on the ratios $\sigma_{cr}^{pl}/\sigma_E$, w_{1i}/b, and I_f/I_t. The ratio $\sigma_{max}/\sigma_{cr}^{pl}$ increases for increasing w_{1i}/b and decreases for increasing I_f/I_t and $\sigma_{cr}^{pl}/\sigma_E$. In the case of columns with small eccentricities with an I_f/I_t ratio of approximately .6 and a $\sigma_{cr}^{pl}/\sigma_E$ ratio greater than .8, there is little increase in the load carrying capacity after the critical load is reached.

(3) The difference between curves representing column action and combined action decreases for increasing initial eccentricity of a column.

As far as design applications are concerned, the most significant finding of this investigation is that there is very little reserve of strength after the critical load is reached. Although this has been proved to be the case only for columns exhibiting the characteristics described in item (2) of the conclusions, it is conceivable that, for other cases as well, there will be a reduction in the load carrying capacity of the column due to local buckling of the component plates. Another important conclusion derived from the present analysis is that

large initial eccentricities in both plate and column lessen the effect of combined action. Consequently, it would be unwise to propose specific design recommendations based on the conclusions of this paper, since actual columns are eccentric and eccentricities play an important role in the behavior of the member. Therefore, it would be necessary to make further investigations before establishing specific limitations in design applications. Some of the possible improvements that could be added to the present analysis are discussed in the next section.

14. Suggestions for Further Investigations

Two possible ways of extending the present solution to include very large deflections in the buckled plates have been indicated in section 11. They consist of adding an extra term for the w deflections of the plates, and the study of the possible change in the buckle pattern of the flanges. The effect of edge restraint is also a factor that could be considered in the selection of the w terms.

Another problem that could also be studied using the Rayleigh-Ritz method is the case in which the side plates buckle. However, the large number of generalized coordinates to be considered in such an analysis increases enormously the labor involved in the computations. An attempt has been made to study the behavior of a square tube of uniform thickness where all four sides buckle simultaneously, and the edges are considered as simply supported. The analysis involved approximately twenty generalized coordinates and the results showed critical loads higher than the Euler load. The generalized coordinates used in the analysis of the square tube to describe the displacements of the flanges, contained terms similar to those used in the present solution. Consequently, it

may be inferred that the selection of the w, u, and v displacements for the side plates is a critical factor in the solution of the problem by the Rayleigh-Ritz method.

A far more complete analysis would involve the determination of the effect of plastic strains on the behavior of the column. For such analysis the variational procedure used by Mayers and Budiansky (8) could be applied in connection with the present elastic solution. It is believed that the labor involved in the computations for such a problem makes its solution unjustifiable if not prohibitive at the present time.

VI BIBLIOGRAPHY

1. Timoshenko, S.: History of Strength of Materials, McGraw-Hill Book Co., Inc., 1953.

2. Bleich, F.: Buckling Strength of Metal Structures, McGraw-Hill Book Co., Inc., 1952.

3. Timoshenko, S.: Theory of Elastic Stability, McGraw-Hill Book Co., Inc., 1936.

4. von Karman, T., Sechler, E. E., and Donnell, L. H.: The Strength of Thin Plates in Compression, A.S.M.E. Trans., APM-54-5, vol. 54, No. 2, 1932.

5. Levy, S.: Bending of Rectangular Plates with Large Deflections, NACA Rep. 737, 1942.

6. Hu, P. C., Lundquist, E. E., and Batdorf, S. B.: Effect of Small Deviations from Flatness on Effective Width and Buckling of Plates in Compression, NACA TN 1124, 1946.

7. Coan, J. M.: Large Deflection Theory for Plates with Small Initial Curvature Loaded in Edge Compression, Jour. Appl. Mech., vol. 18, No. 2, 1951.

8. Mayers, J., and Budiansky, B.: Analysis of Behavior of Simply Supported Flat Plates Compressed Beyond the Buckling Load Into the Plastic Range, NACA TN 3368, 1955.

9. Stein, M.: Behavior of Buckled Rectangular Plates, Journal of the Engineering Mechanics Division, ASCE Proceedings, vol. 86, No. EM 2, 1960.

10. Duberg, J. E., and Wilder III, T. W.: Inelastic Column Behavior, NACA TN 2267, 1951.

11. Bijlaard, P. P., and Fisher, G. P.: Interaction of Column and Local Buckling in Compression Members, NACA TN 2640, 1952.

12. Bijlaard, P. P., and Fisher, G. P.: Column Strength of H-Sections and Square Tubes in the Post-Buckling Range of Component Plates, NACA TN 2994, 1953.

13. Langhaar, H. L.: General Theory of Buckling, Applied Mechanics Review, vol. 11, 1958.

14. Langhaar, H. L., and Boresi, A. P.: Snap-Through and Post-Buckling Behavior of Cylindrical Shells Under Action of External Pressure, University of Illinois Eng. Exp. Sta., Bul. 443, 1957.

15. Love, A. E. H.: A Treatise on the Mathematical Theory of Elasticity, Dover Publications, 1944.

16. Scarborough, J. B.: Numerical Mathematical Analysis, Oxford University Press, 1955.

17. Crandall, S. H.: Engineering Analysis, McGraw-Hill Book Co., Inc., 1956.

APPENDIX I

Column Action

When $w_a = w_b = 0$ the problem reduces to column action. In this case Eqs. (16) through (30) simplify into,

$$\frac{u_0}{L} - 2\pi K_1 - \frac{\sigma}{E} = 0 \tag{26.a}$$

$$\frac{u_3}{L} + K_1 = 0 \tag{27.a}$$

$$H_3 + \frac{w_0}{L}\left(1 + \frac{b_1}{b}\frac{t_1}{t}\right)\left(\pi\frac{u_3}{L} - \frac{u_0}{L} + 3\pi K_1\right) = 0 \quad . \tag{28.a}$$

The above system of equations reduces to the well known relation,

$$\frac{w_0}{L} = \frac{w_{0i}}{L} \frac{1}{1 - \frac{\sigma}{\sigma_E}} \quad . \tag{35}$$

where

$$\sigma_E = \pi^2 \frac{EI_t}{AL^2} \quad .$$

It should be mentioned that there is no error introduced by assuming Poisson's ratio equal to zero. The computer solution coincides with Eq. (35).

APPENDIX II

Plate Action

When $w_0 = u_3 = 0$ and the ratio t_1/t is taken equal to zero, the problem reduces to plate action. In this case $w_a = w_b$ and Eqs. (16) through (30) simplify into,

$$\frac{v_{11}}{b} + 2\pi I_1 = 0 \tag{16.b}$$

$$\frac{v_{31}}{b} + I_1 = 0 \tag{18.b}$$

$$\frac{3}{2}\frac{v_{41}}{b} + \frac{1}{2}\frac{u_{21}}{b} + I_1 = 0 \tag{20.b}$$

$$\frac{u_{11}}{b} + I_1 = 0 \tag{22.b}$$

$$\frac{3}{2}\frac{u_{21}}{b} + \frac{1}{2}\frac{v_{41}}{b} + 2I_1 = 0 \tag{24.b}$$

$$-\frac{1}{4}\frac{u_0}{L}\frac{w_a}{b} + J_6 + \frac{5}{2}\pi\frac{w_a}{b} I_1 + H_5 = 0 \quad . \tag{29.b}$$

The solution of the above system of equations leads to results that agree very closely with those of a more exact theory by Hu, Lundquist, and Batdorf (6). The results are depicted in Figs. 4 and 5. They show that the effect of Poisson's ratio in the load-displacement curves is not appreciable since the results presented by Hu, Lundquist, and Batdorf (6) have been obtained for $\nu = .316$ as compared to $\nu = 0$ used in the present energy solution. It should be pointed out that although the expressions for the displacements agree very well with the more rigorous solution, it could be expected that the surface strains computed from the displacements expressions entail appreciable errors since they depend on the second derivative of the assumed deflected shape.

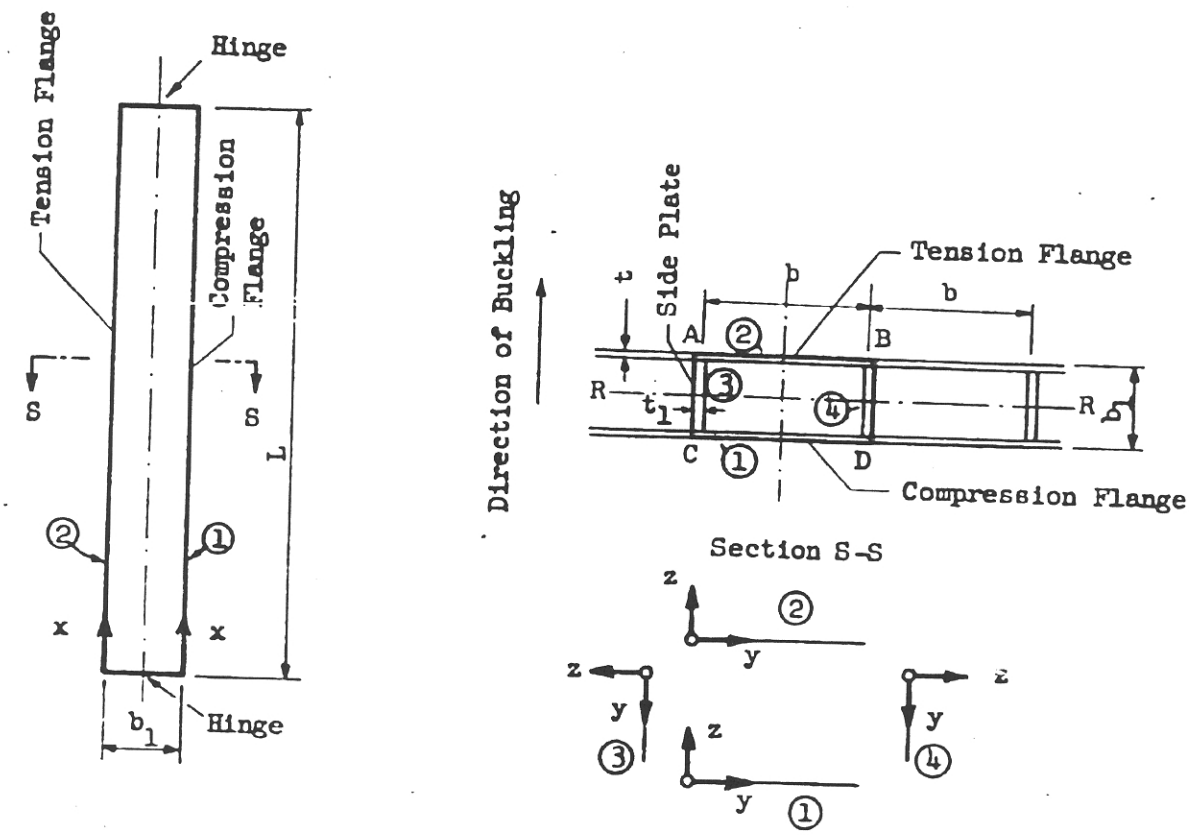

Fig. 1 Geometry and Coordinates

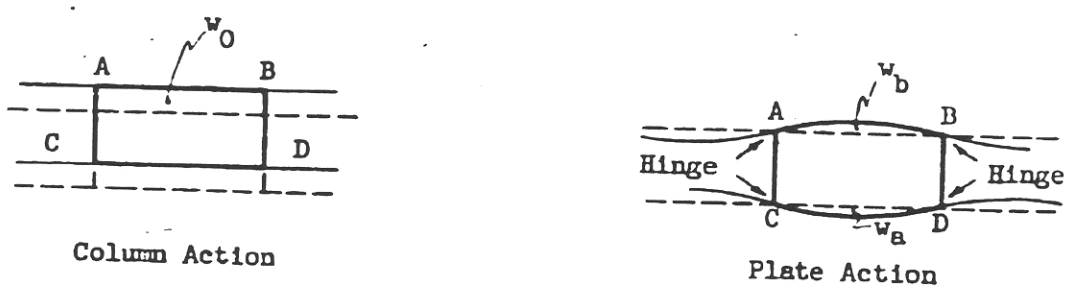

Fig. 2 Assumed Lateral Deflections of the Middle Cross Section of the Column

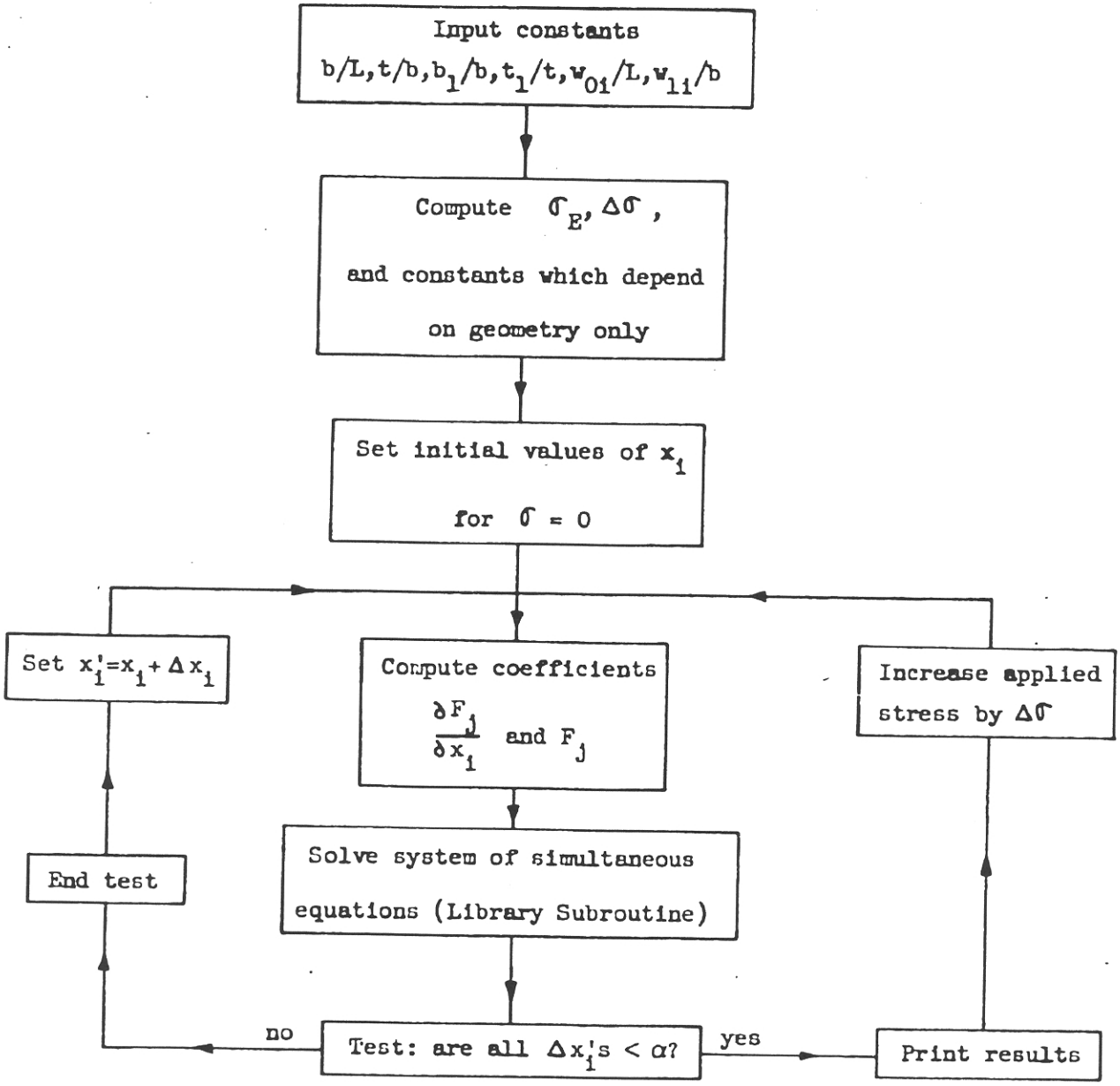

Fig. 3 Simplified Flow Diagram

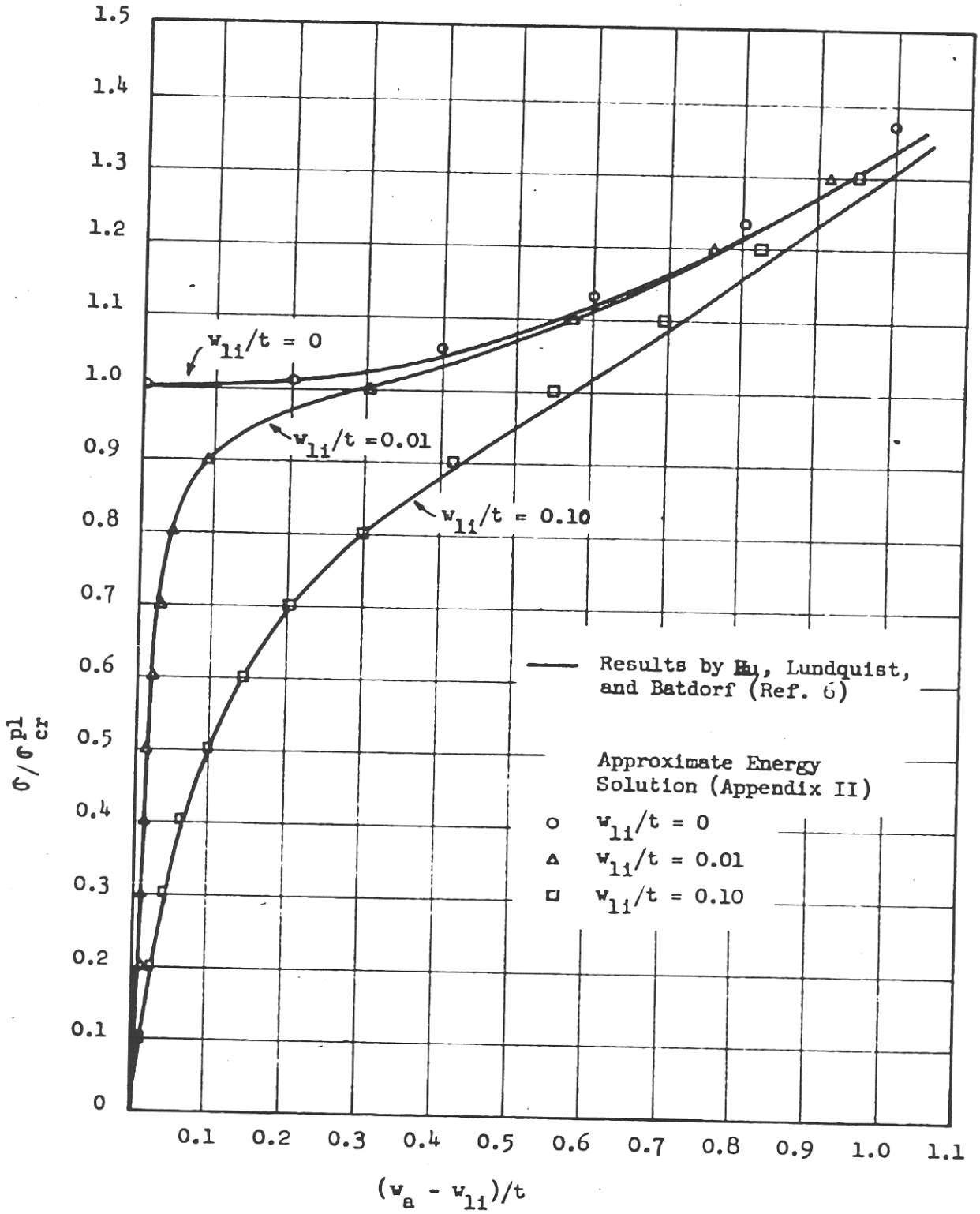

Fig. 4 Plate Action: Variation of Net-Buckle-Crest-Deflection Ratio With the Ratio σ/σ_{cr}^{pl}, for a Simply Supported Square Plate

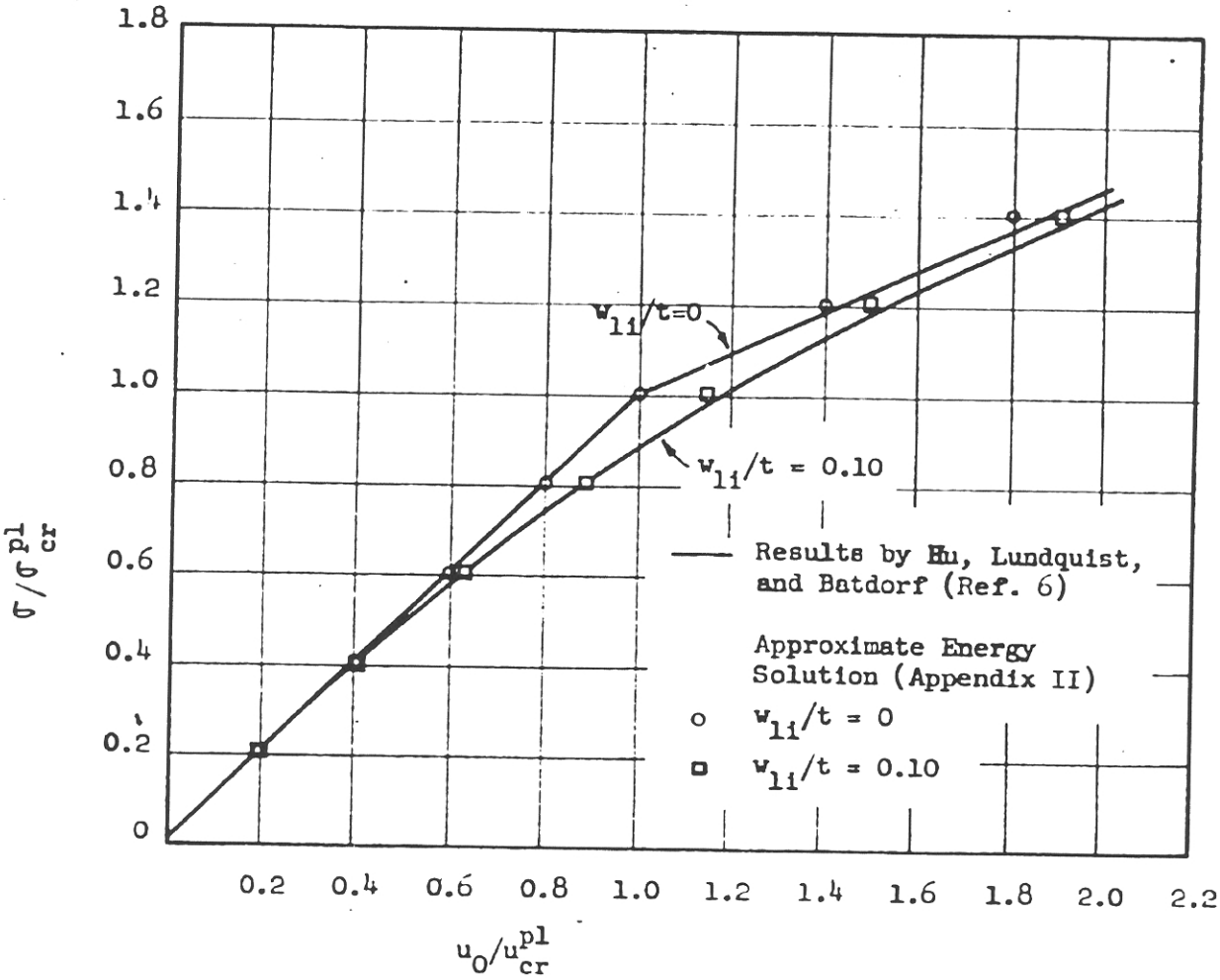

Fig. 5 Plate Action: Variation of the Plate Shortening Ratio With the Ratio σ/σ_{cr}^{pl}, for a Simply Supported Square Plate

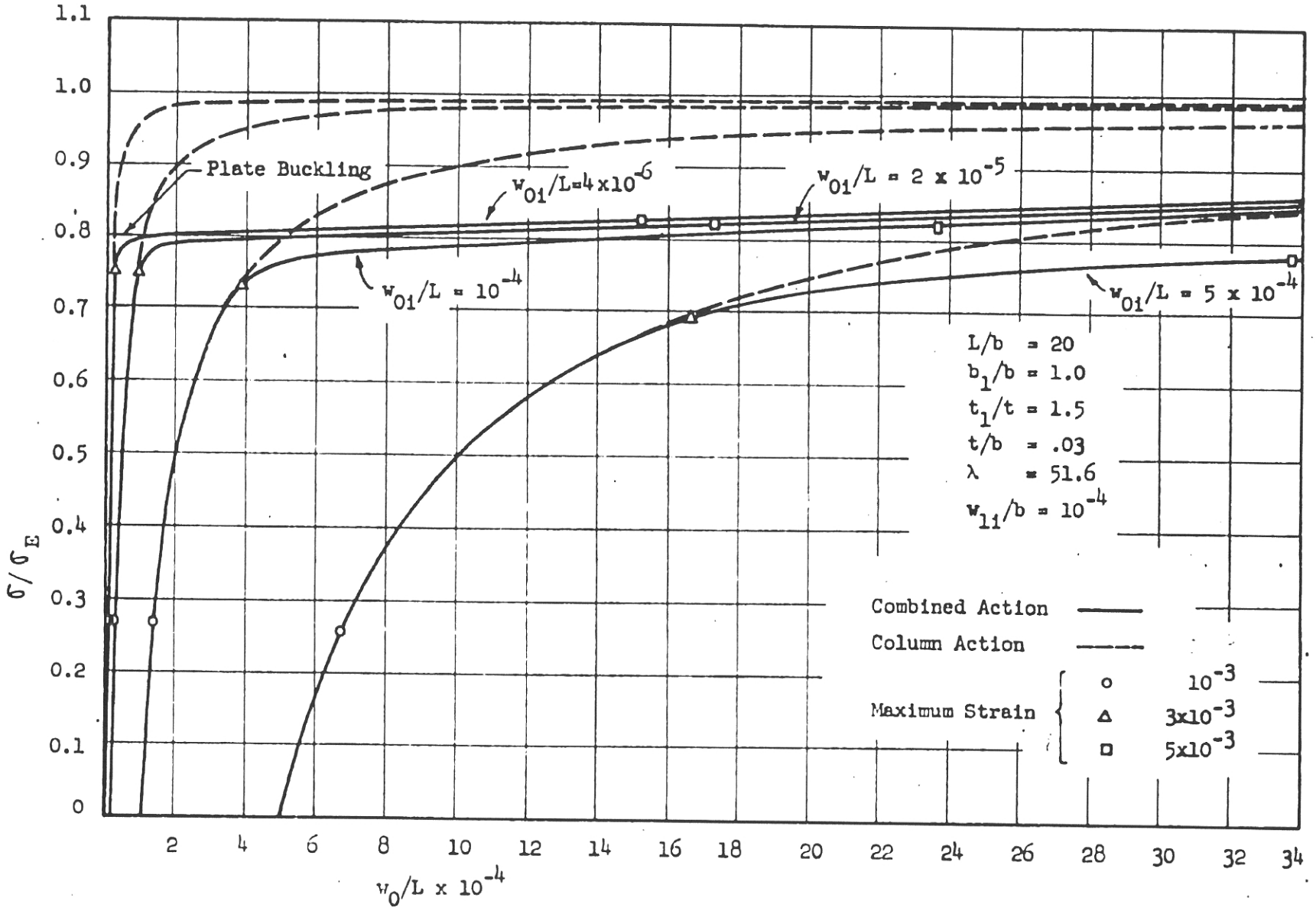

Fig. 6 Variation of the Ratio w_0/L With σ/σ_E, for Different Column Eccentricities (L/b = 20)

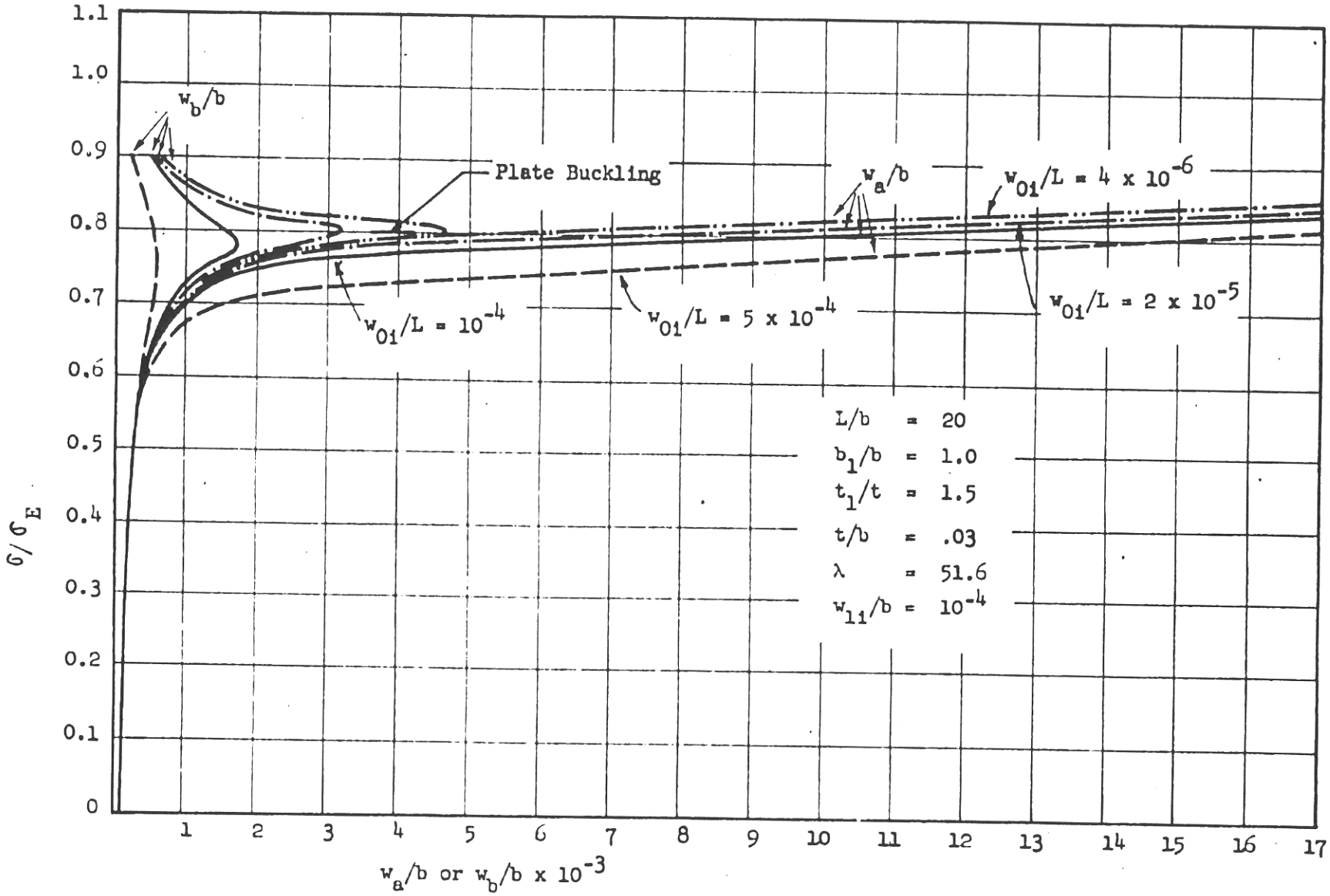

Fig. 7 Variation of the Buckle-Crest-Deflection Ratio of the Compression and Tension Flanges With σ/σ_E, for Different Column Eccentricities ($L/b = 20$)

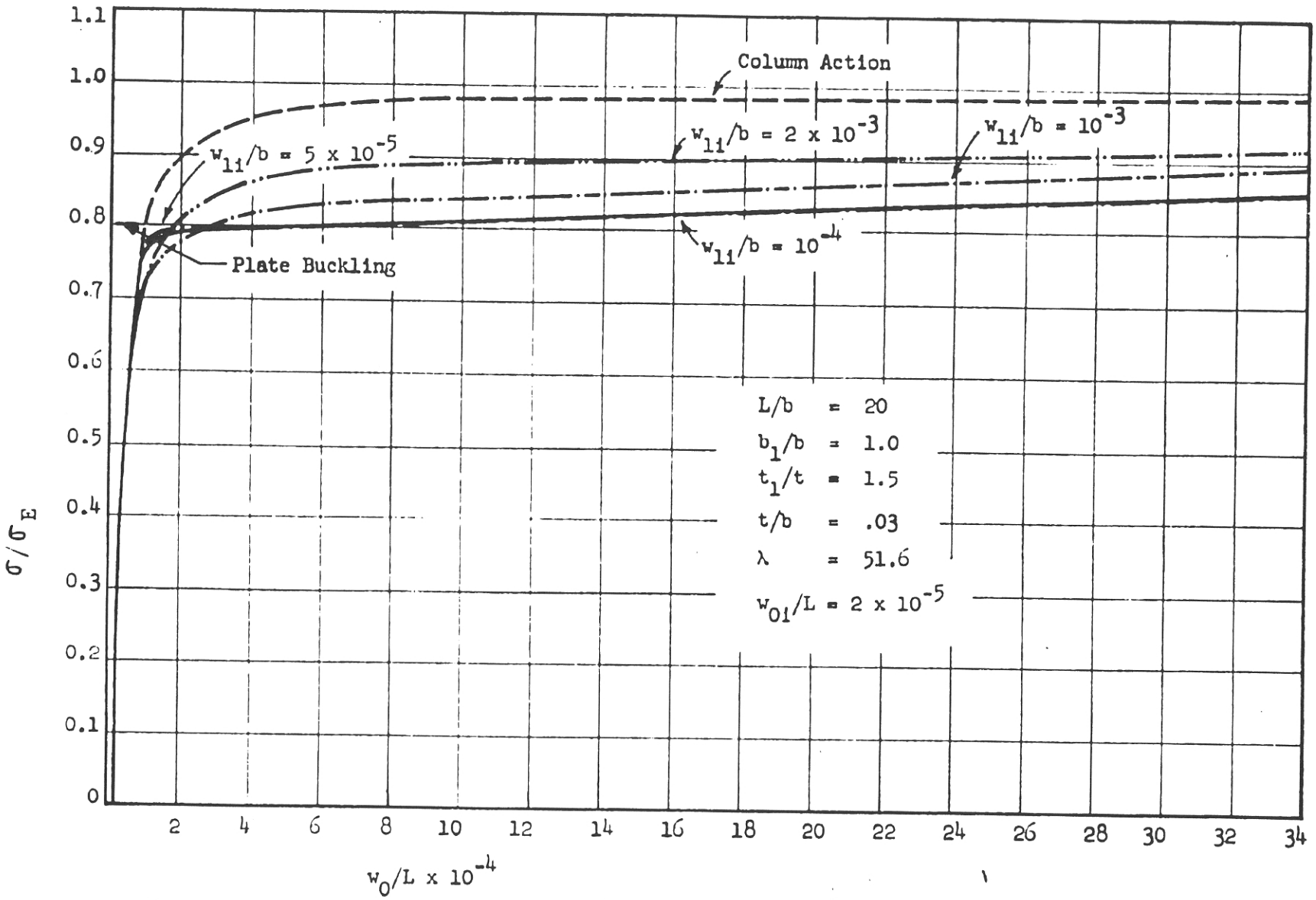

Fig. 8 Variation of the Ratio w_0/L With σ/σ_E, for Different Plate Eccentricities (L/b = 20)

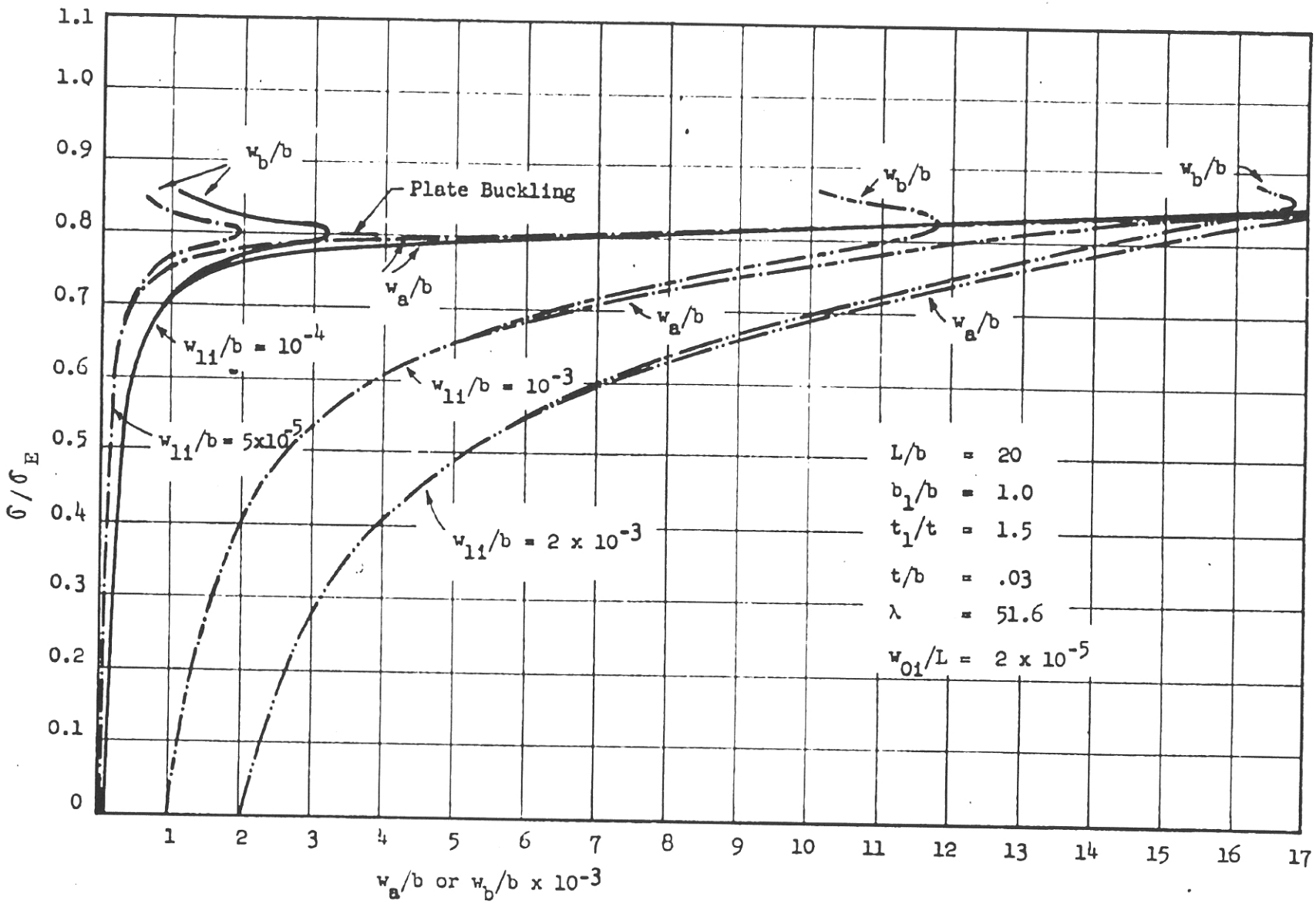

Fig. 9 Variation of the Buckle-Crest-Deflection Ratio of the Compression and Tension Flanges With σ/σ_E, for Different Plate Eccentricities (L/b = 20)

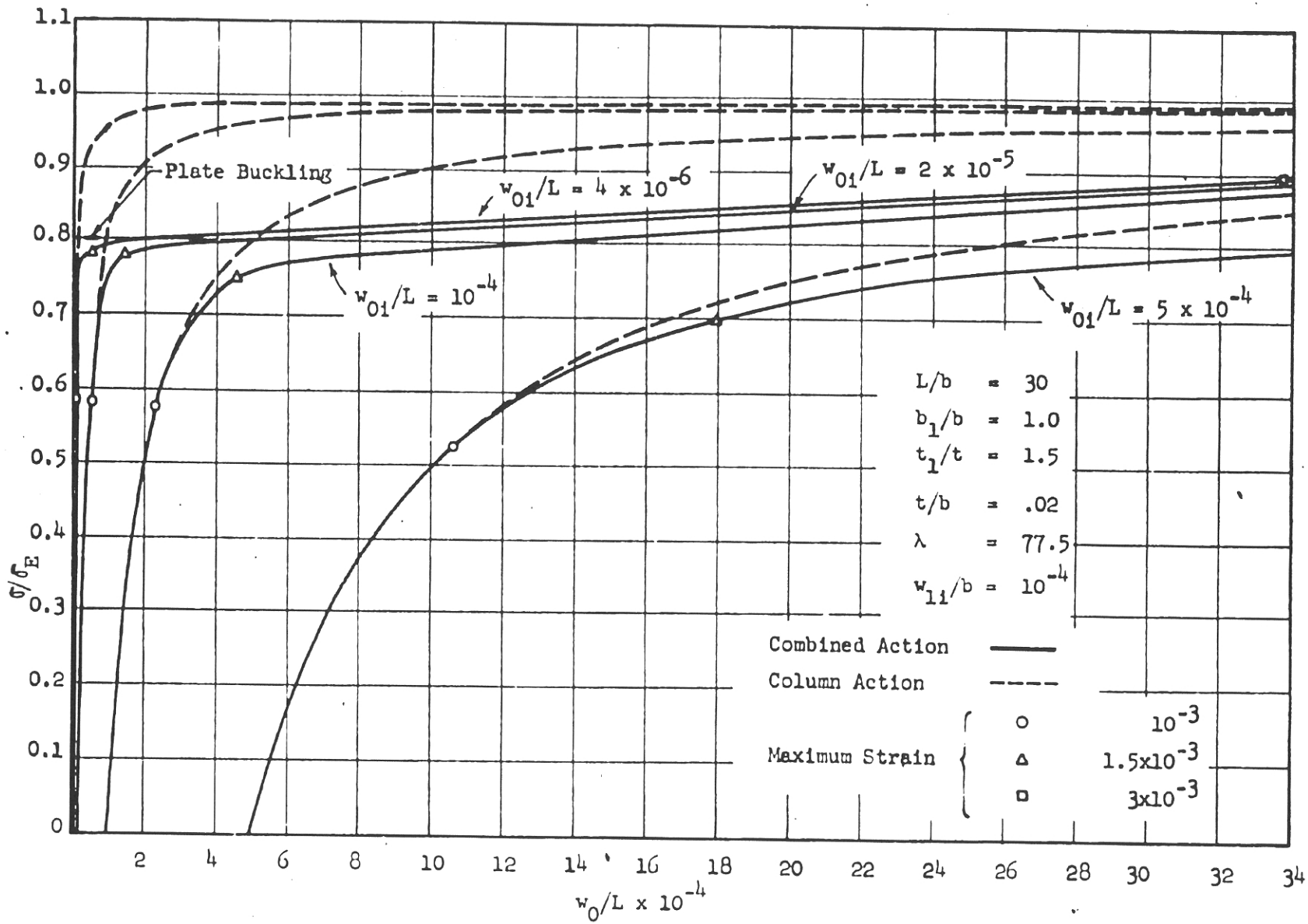

Fig. 10 Variation of the Ratio w_0/L With σ/σ_E, for Different Column Eccentricities (L/b = 30)

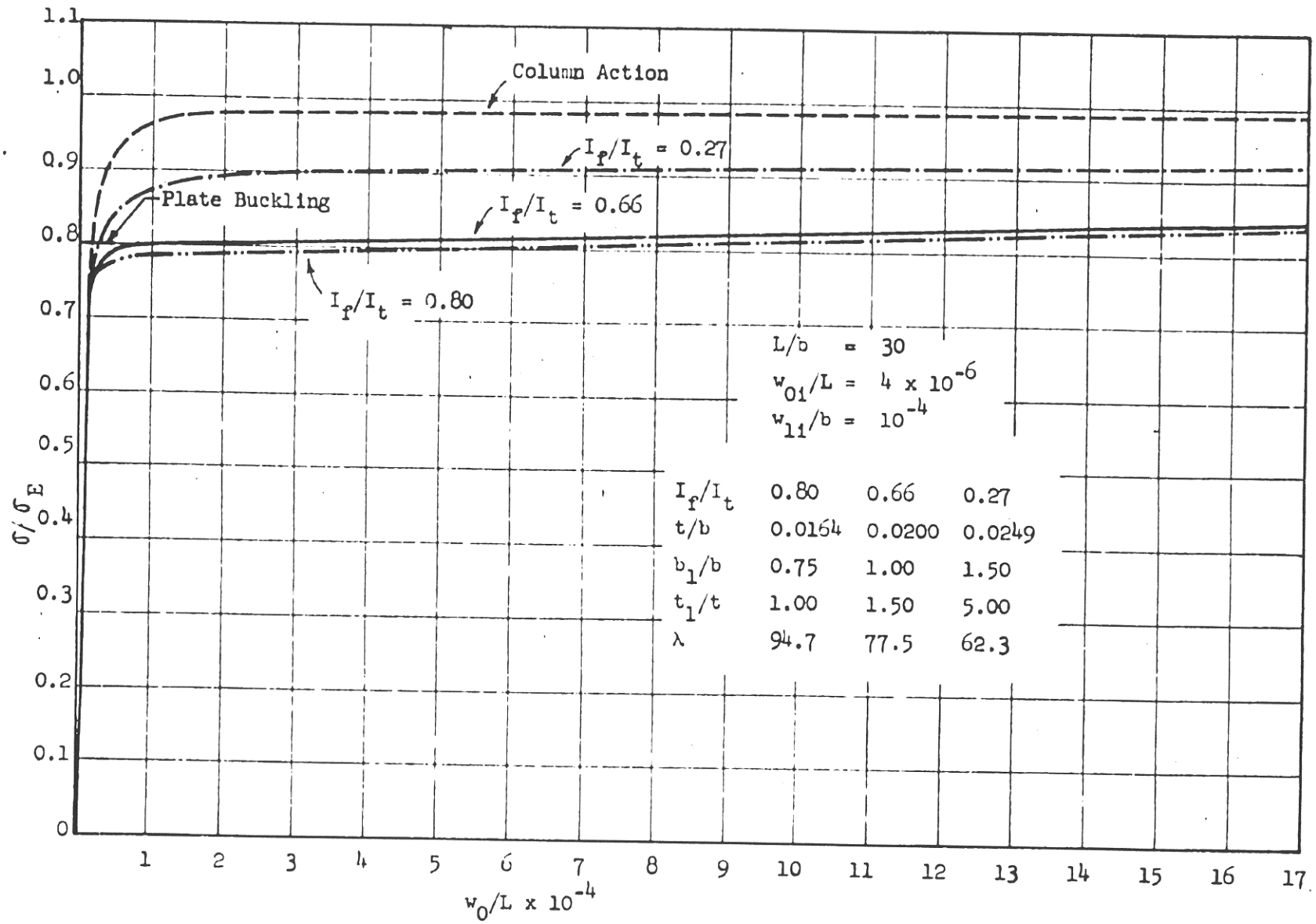

Fig. 11 Variation of w_0/L With σ/σ_E, for Different I_f/I_t Ratios (L/b = 30)

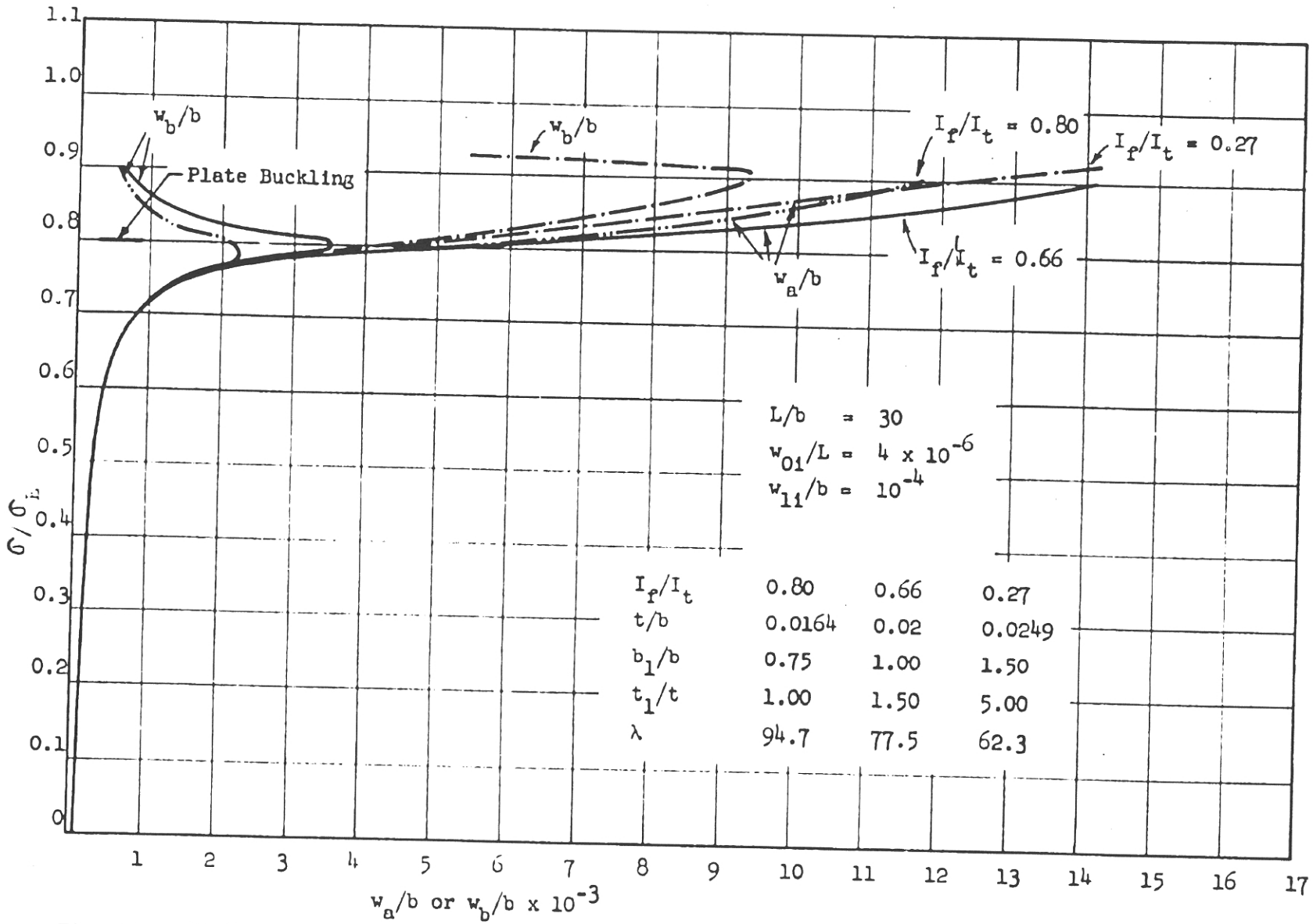

Fig. 12 Variation of the Buckle-Crest-Deflection Ratio of the Compression and Tension Flanges With σ/σ_E, for Different I_f/I_t ($L/b = 30$)

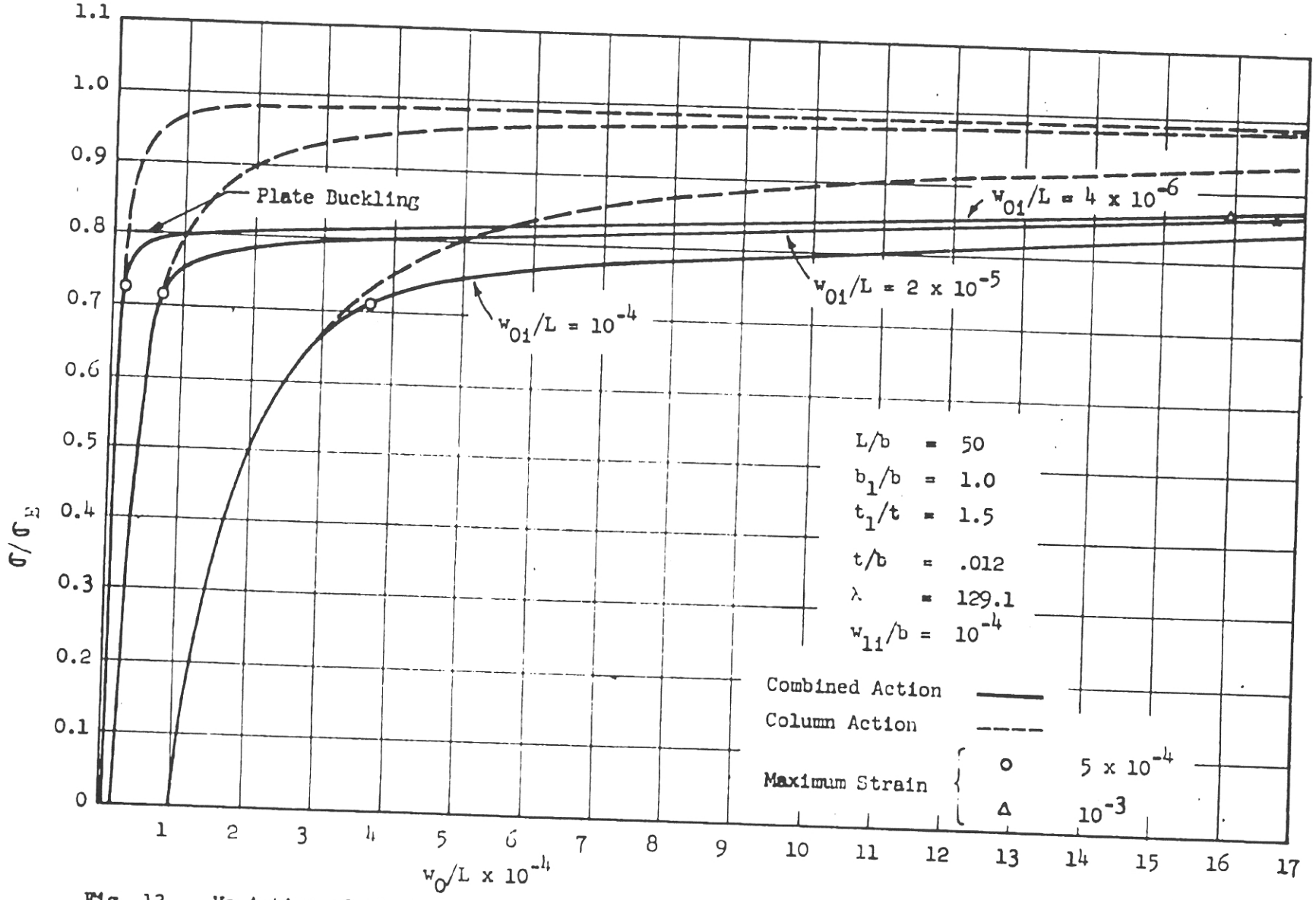

Fig. 13 Variation of the Ratio w_0/L With σ/σ_E, for Different Column Eccentricities (L/b = 50)

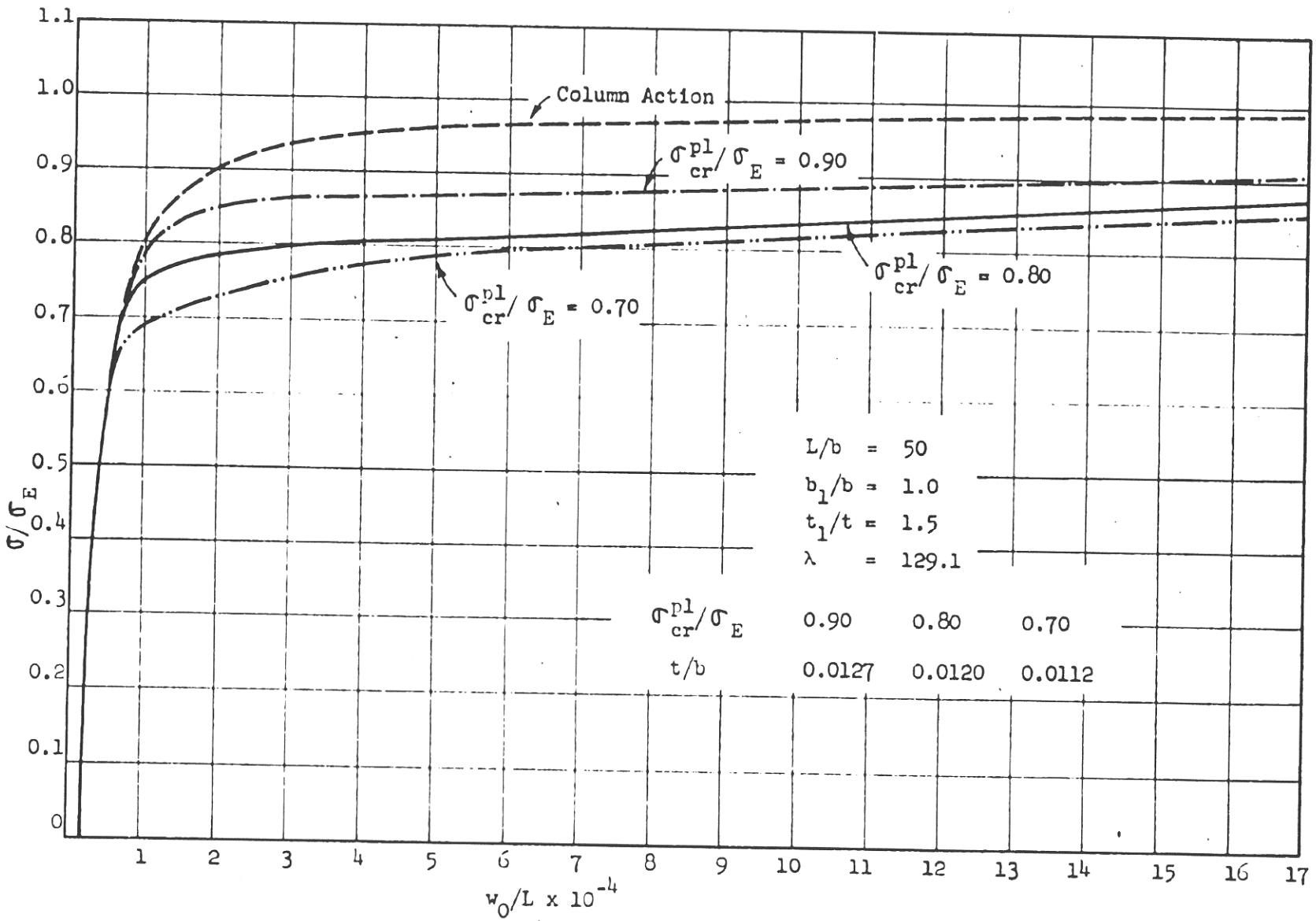

Fig. 14 Variation of the Ratio w_0/L With σ/σ_E, for Different $\sigma_{cr}^{pl}/\sigma_E$ Ratios (L/b = 50)

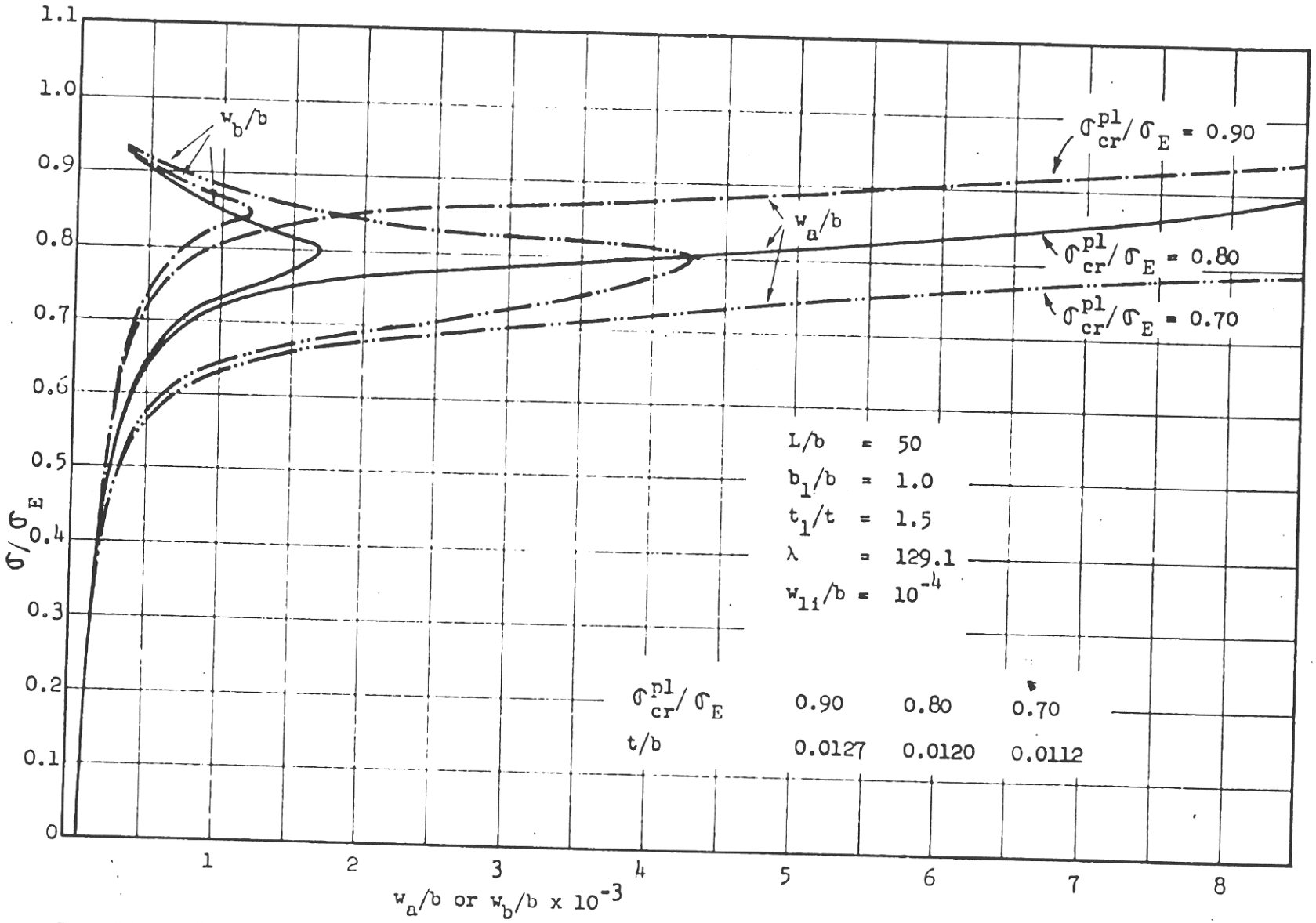

Fig. 15 Variation of the Buckle-Crest-Deflection Ratio of the Compression and Tension Flanges With σ/σ_E, for Different $\sigma_{cr}^{pl}/\sigma_E$ (L/b = 50)

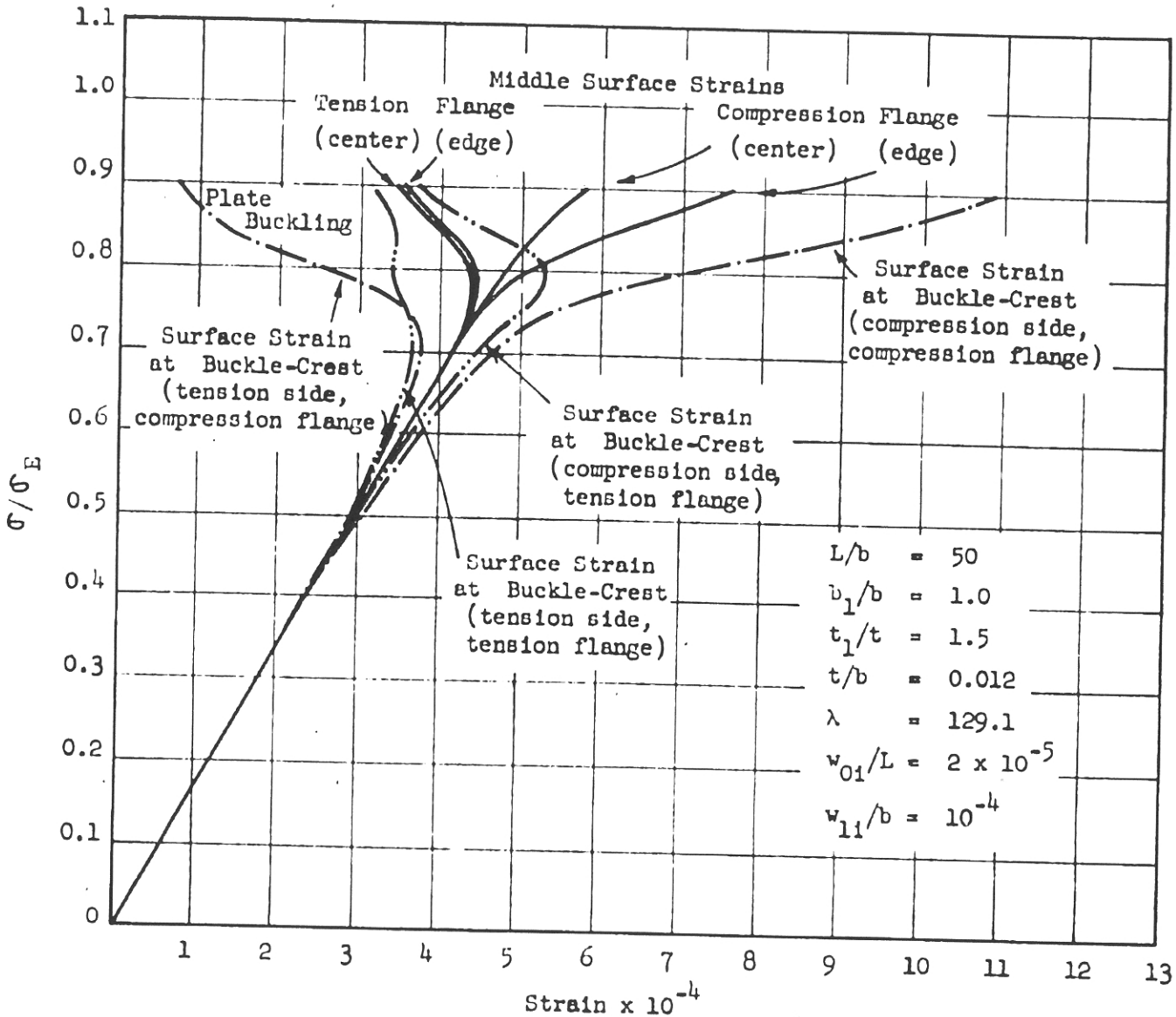

Fig. 16 Longitudinal Strains at Middle Cross Section of the Column (L/b = 50)

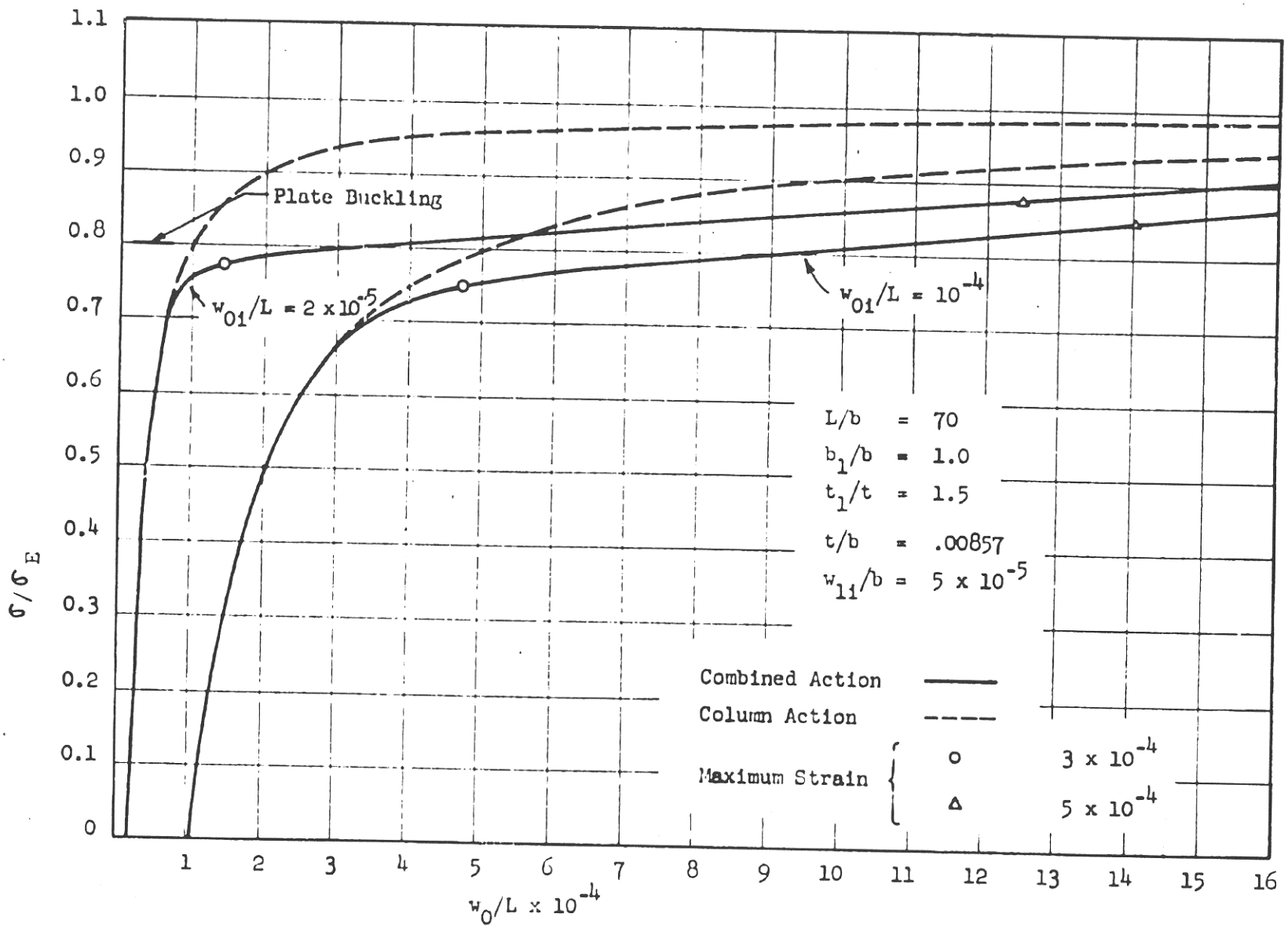

Fig. 17 Variation of the Ratio w_0/L With σ/σ_E, for Different Column Eccentricities (L/b = 70)

VITA

Jacques Cohen was born in Belo Horizonte, Brazil, on November 13, 1932. He obtained his secondary education at the Colegio Estadual de Minas Gerais, Belo Horizonte, graduating in 1950.

In March 1951 he entered the Escola de Engenharia da Universidade de Minas Gerais, Belo Horizonte. In 1955 he received the B.S. degree in Civil Engineering from that University. He was the recipient of the Arthur Guimaraes Award, as the first student in the graduating class. He also won a scholarship sponsored by the Escola de Engenharia da Universidade de Minas Gerais for graduate study in the United States of America.

In the period 1955-1956 he worked as a structural engineer in a steel structures company located in Belo Horizonte.

He was a graduate student at the University of Florida from September 1956 to February 1958, receiving the degree of Master of Science in Engineering. In February 1958 he entered the University of Illinois to continue graduate work in Civil Engineering.

He holds membership in Phi Kappa Phi, American Society of Civil Engineers, American Concrete Institute, and is a registered Civil Engineer in Brazil.